AN ELECTRON IMPACT STUDY OF CARBON MONOXIDE

Dissertation

Presented in Partial Fulfillment of the Requirements
for the Degree Doctor of Philosophy in the
Graduate School of The Ohio State
University

by

Sam Silverman, B. Ch.E.
The Ohio State University -
1952

Approved by:

E. N. Lassettre
Adviser

TABLE OF CONTENTS:

TABLES:

TABLES (CONTINUED):

ILLUSTRATIONS

ILLUSTRATIONS (CONTINUED):

ACKNOWLEDGMENT

In the course of this research, aid was received from many sources. I should like to express my gratitude to:

Dr. E. N. Lassettre, for his constant encouragement and many helpful suggestions;

M. E. Krasnow, in conjunction with whom much of the construction and testing were done;

The Ohio State University, for various teaching assistantships;

The Graduate School, for an appointment as University Scholar;

The Ohio State Research Foundation, for an appointment as Research Assistant during the latter phases of this work;

The members of the Chemistry Department Machine Shop, for their constant help and many valuable suggestions during the construction of the new spectrometer;

My wife, for her patience and for the editing and typing of this dissertation.

I. INTRODUCTION

The investigation described in this thesis initially had two objectives. The first was the construction and testing of a new electron spectrometer which was designed as an improvement over the one previously used in this laboratory. The second was a comparison of the electron impact energy spectra of nickel carbonyl with those of carbon monoxide and several ketones in order to gain additional information about the character of the carbon-oxygen bond in the nickel-carbonyl molecule. This latter objective was superseded by a thorough quantitative study of the collision cross sections and energy spectra of carbon monoxide. This was done because of the greater interest attached to the carbon monoxide molecule, especially in view of the fact that a concurrent investigation in this laboratory was being carried out on the nitrogen molecule by M. E. Krasnow. A comparison between these two molecules is important because of the marked similarity of physical properties and the fact that the bond structures are not yet thoroughly understood. Thus any evidence leading toward an elucidation of these characteristics is significant.

Some work on electron scattering by carbon monoxide has been reported in the literature and will be described briefly.

Several workers (1) (2) have investigated the critical potentials, including one study (3) by the retarding potential method, using incident electrons of 5.2 volts energy.

Absorption coefficients have been determined for incident electron energies under 10 volts by Lohner (4), Brose and Saayman (5), and Ramsauer and Kollath (6), for electron energies up to about 45 volts by Bruche (7), and for electron energies up to 225 volts by Brode (8).

Normand (9) has studied the total absorption coefficient as a function of incident electron energy from 0.5 to 400 volts. He reports total absorption coefficients, α, of approximately 16 at 256 volts, approximately 13 at 324 volts, and approximately 12 at 400 volts.

Rudberg (10) (11) carried out an investigation of the energy spectra of carbon monoxide at zero scattering angle. He reports excitation potentials at 8.19, 11.17, 13.24, 16.72, and 21.90 volts. His interpretation of these spectra is, however, open to some question.

Kollath (12) has studied the elastic scattering at 90 degrees for incident electron energies up to 36 volts. Ramsauer and Kollath (13) studied the angular distribution of

scattered electrons from 15 to 167 degrees for electrons with energies between one and six volts.

Arnot (14) has studied the elastic scattering between 20 and 120 degrees for incident electron energies from 30 to 800 volts. He reports a steady decrease in intensity as the scattering angle is increased with no maxima or minima apparent.

Mulliken (15) has discussed the ultraviolet spectra and the electronic configuration of the ground state. Moffitt (16) has given a theoretical molecular orbital treatment of both the ground state and first excited state.

II. Experimental Method

A. The Electron Spectrometer

The electron spectrometer used in the present investigation is an improved version of one which has been described by previous workers (17), (18), (19), (20), (21), (22), (23) in this laboratory.

The revision of the spectrometer is primarily due to Doctors E. N. Lassettre and A. S. Berman, and was undertaken to provide increased resolving power and a higher sensitivity in the measurement of scattered current. A detailed description of the apparatus will be given since none has been reported elsewhere.

The general operating principles of the instrument are given schematically in Figure 1. An electron gun, G, serves as the source of an electron beam which is passed through the gas, maintained at a definite pressure, as measured by a Knudsen Gauge, in the collision chamber C. Those electrons which are deflected through an angle, θ, pass through the slit system, S_1 and S_2, into the parallel plate electrostatic analyzer, A. Here, a velocity analysis is performed by varying the potential between plates P_1 and P_2. Electrons with an energy defined by this potential then pass through slits S_3 and S_4, into an electron multiplier. For each

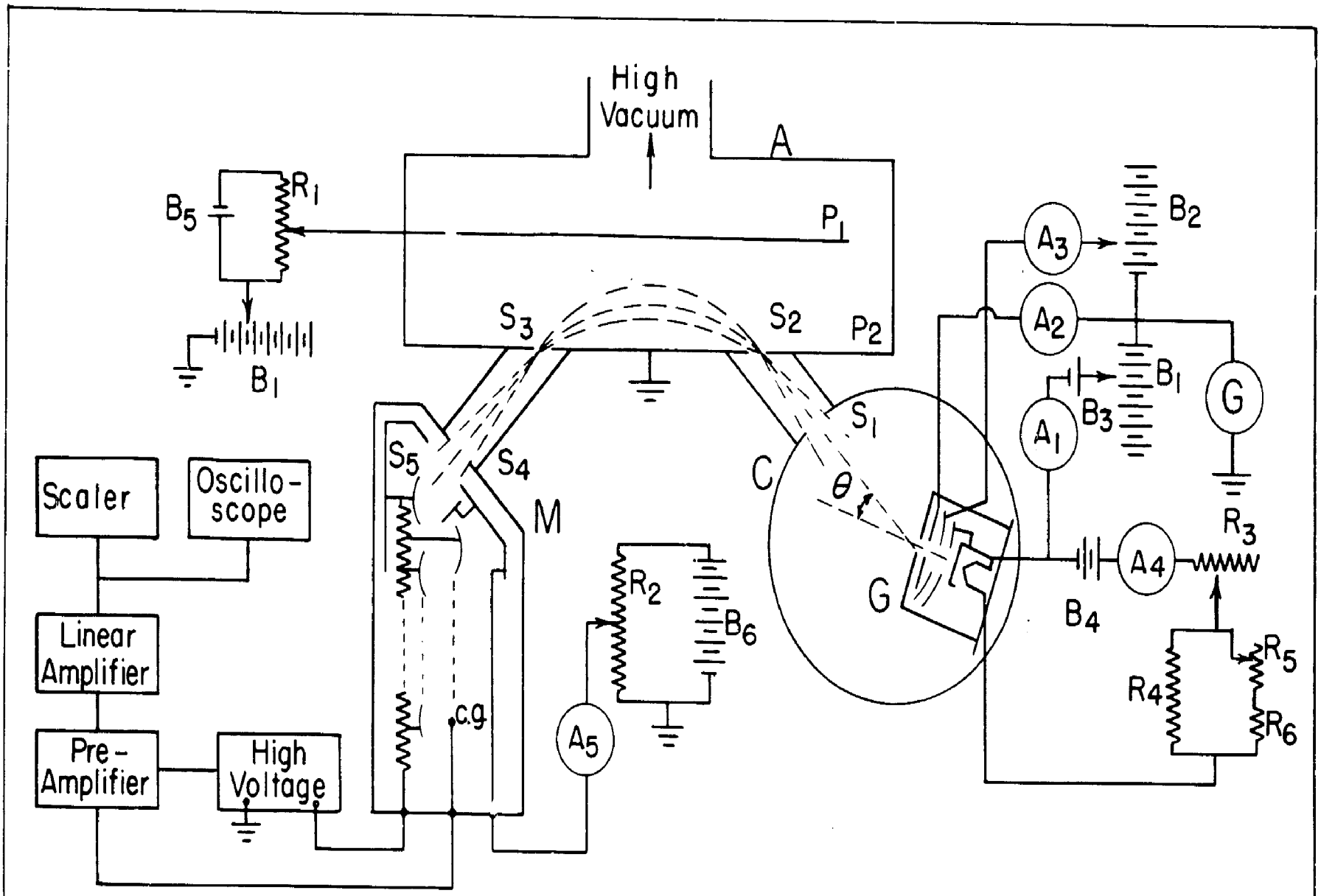

Figure 1

SCHEMATIC REPRESENTATION OF ELECTRON SPECTROMETER

electron entering, approximately 10^6 are collected on the collector grid, c.g., producing a pulse which is amplified by the pre-amplifier and a fast linear amplifier and counted on a multiscaler. A monitoring oscilloscope is used for checking on the pulse shapes and heights.

Figures 2 and 3 show in greater detail the electrical control and measurement circuits associated with the spectrometer, and Table 1 gives a complete parts list for these circuits. These will be used in conjunction with Figure 1 in the detailed description which follows.

(a) Pumping systems and vacuum:

A Kinney Type CVD556 rotary oil pump is used to bring the pressure in the system from atmospheric pressure down to about 20 microns. A National Research Corporation high speed oil diffusion pump, Type H6P, provides the additional pumping needed to reach an operating pressure in the range of 3×10^{-6} mm. Hg.

Two additional features of the new apparatus may be mentioned here. These are: (a) a means for changing emitters while the analyzer and multiplier are kept under vacuum, and (b) a separate evacuation of the electron gun to minimize the effect of the gas being studied on the oxide coated cathode. The former objective is achieved by having a cut-off valve

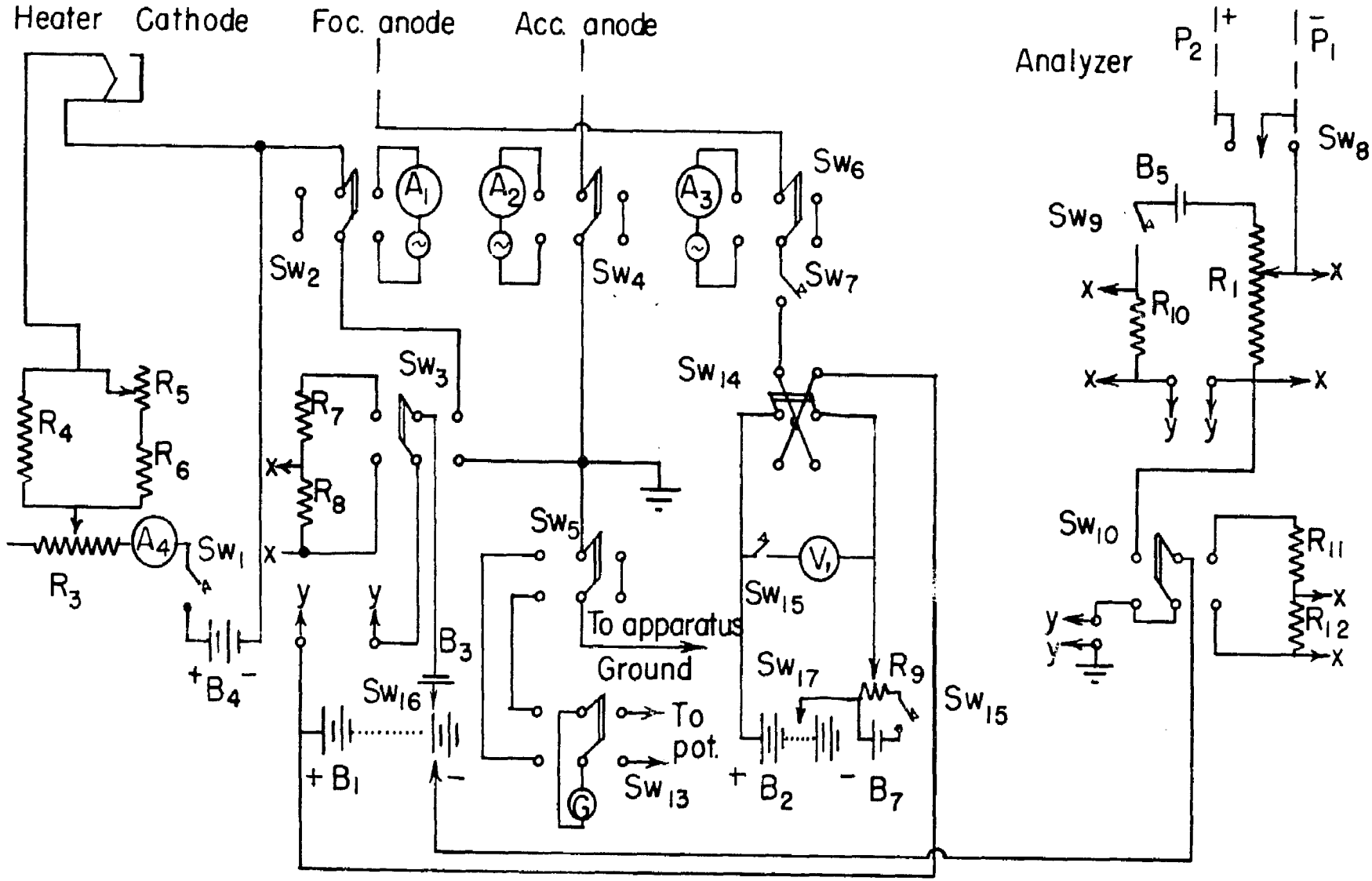

x-x To potentiometer selector switch, Sw_{11}

y-y To meter insertion switch, Sw_{12}

ELECTRICAL CIRCUITS OF ELECTRON SPECTROMETER

Figure 2

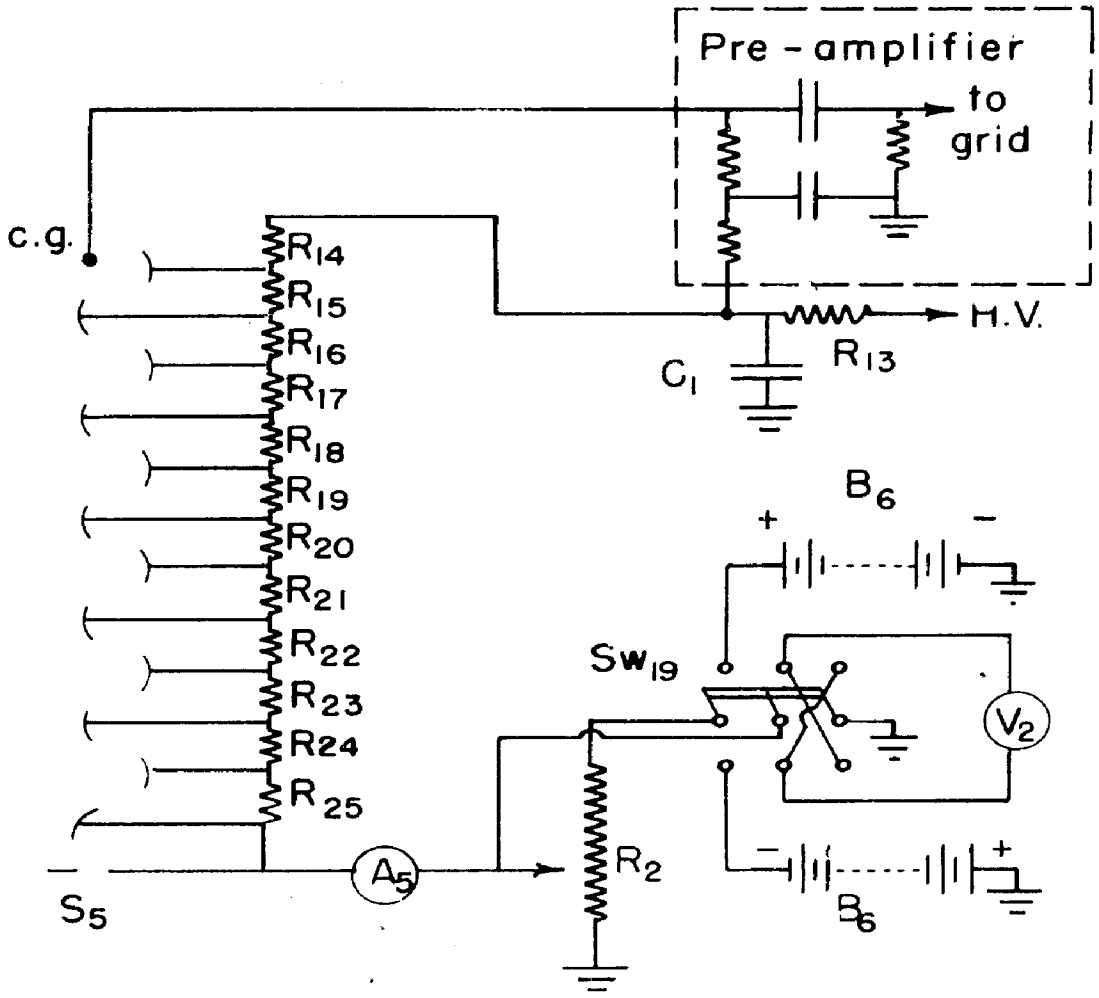

ELECTRICAL CIRCUITS — ELECTRON MULTIPLIER

Figure 3.

Table 1.

PARTS LIST FOR ELECTRON SPECTROMETER

Resistors:

R_1	100,000ohm Helipot, 15 turns
R_2	2 megohm, volume control potentiometer
R_3	12 ohm, 50 watt, ohmite rheostat
R_4	10 ohm, 20 watt, ohmite "Brown Devil"
R_5	5 ohm Helipot, three turns
R_6	5 ohm, 10 watt, ohmite "Brown Devil"
R_7, R_{11}	1 megohm, precision wire wound
R_8, R_{10}, R_{12}	1000 ohms standard resistor, General Radio
R_9	80,000 ohm potentiometer
R_{13}-R_{25}	9.1 megohm

Meters:

A_1, A_3, A_5	D. C. Microammeter, 0 - 100
A_2	D. C. Microammeter, 0 - 150
A_4	D. C. Ammeter, 0 - 5
A_6	D. C. Milliammeter, 0 - 1 (for use with meter insertion switch, Sw_{12}, not shown in diagram)
V_1, V_2	D. C. Volt meter, 0 - 500
G	Galvanometer and Ayrton Shunt

Table 1. (cont.)

Condenser:

C_1	1 microfarad

Switches:

Sw_1, Sw_7, Sw_9	Single pole, single throw toggle switch
Sw_2, Sw_3, Sw_4, Sw_5, Sw_6, Sw_{10}, Sw_{13}, Sw_{14}	Double pole, double throw, General Radio
Sw_8	Single pole, double throw toggle switch
Sw_{11}	Two circuit, five position
Sw_{12}	Meter Insertion Switch, Yaxley no. 1400
Sw_{15}	Double pole, double throw toggle switch
Sw_{16}	Rotary Selector Switch
Sw_{17}	Rotary Selector Switch, Mallory Type 176C
Sw_{18}	Double pole, double throw General Radio (in accelerating volts circuit to switch in additional 22 1/2 volt battery -- not shown in diagram)
Sw_{19}	Four pole, double throw General Radio

Batteries:

B_1	Power Pack, Twelve 45 volt B - batteries
B_2	Power Pack, Ten 45 volt B - batteries
B_3, B_5, B_7	45 volt B - battery
B_4	Two 6 volt storage batteries
B_5	Power Pack, Fourteen 45 volt B - batteries

between collision chamber, C, and analyzer, A, and by-pass lines to the forepump and oil diffusion pump. A low pressure in the electron gun is maintained by means of a National Research Corporation Type H2P oil diffusion pump, using the Kinney Pump mentioned above in the fo: epressure line. Since gas flow between collision chamber and gun occurs only through the electrode apertures, a pressure differential of ten times or more is possible.

National Research Corporation Type 501 Thermocouple gauges and Type 507 Ionization gauges are mounted in the analyzer and collision chamber top. An additional thermocouple gauge is in the line to the Kinney Pump. For convenience in leak detection, ionization gauges are also located in the multiplier and in the manifold leading to the collision chamber. All these gauges are used with a switching device and a National Research Corporation Type 710 Control.

A Knudsen gauge is used to measure gas pressure in the collision chamber, since the response of this type of gauge is independent of the nature of the gas. The gauge was calibrated by M. E. Krasnow and will be treated in detail in his thesis.

(b) Electron Gun:

The electron gun, G, is contained in a housing mounted on a ball bearing race on the top of the collision chamber and can be rotated, relative to the collision chamber and slit systems, through any angle, θ, up to ninety degrees, by means of a worm gear with a scale graduated in minutes. Two O-Rings are used as vacuum seals, the space between them being evacuated by a Welch Duo-Seal Pump. It was found that in rotary motion, the standard neoprene O-Rings seize in a very short time. A very satisfactory arrangement eliminating this difficulty is the use of a Buna-N O-Ring, lubricated with Apiezon N grease and Molykote, on the inside and a Silicone O-Ring, lubricated with Apiezon N grease, on the outside.

The emitter is of the indirectly heated type. A heating current of 0.4 to 0.7 amperes, measured by an ammeter, A_4, is obtained by means of storage batteries, B_4, and controlled by a coarse resistance, R_3, and the resistance network, R_4, R_5, and R_6. The fixed resistors, R_4 and R_6, limit the current through the three-turn Helipot, R_5, which serves as the fine control in the filament heating circuit.

The accelerating voltage between cathode and accelerating anode is obtained from a set of B batteries, B_1, which is also used as the analyzer voltage supply, and an additional 45 volt battery, B_3, in series with it. A rotary Selector switch, Sw_{16}, is used to choose any voltage from 90 to 600 volts and an additional switch, Sw_{18} (not shown in the Figure), is used to add 22 1/2 volts. This voltage may be applied directly by using switches, Sw_2, Sw_3, and Sw_4 to bypass the measuring circuits. Microammeters, A_1 and A_2, are available for the measurement of the emission current and the current collected by the accelerating anode, respectively. For an accurate measurement of the accelerating voltage, the e.m.f. developed across the standard 1000 ohm resistance, R_8, which is in series with a wire wound one megohm resistor, R_7, is applied to a Leeds and Northrup Type K potentiometer. A selector switch, Sw_{11}, makes it possible to use this same potentiometer for the measurement of all accelerating and analyzer voltages, and another switch, Sw_{12}, makes feasible the use of a single galvanometer, G, for the measurement of beam current and as the potentiometer null indicator. A coarse voltage measurement is obtained by placing a milliammeter, A_6, in series with the resistors, R_7 and R_8. This meter, used in conjunction with a meter insertion switch, Sw_{12}, is also used for

coarse measurements of analyzer voltages.

During the developmental work on the apparatus, it was found necessary, in order better to collimate the beam, to use both positive and negative focussing voltages. A rotary Selector switch, Sw_{17}, wired to the battery power pack, B_2, is used as a coarse control giving steps of 45 volts. An additional 45 volt battery, B_7, is connected across the potentiometer, R_9, which serves as a fine voltage control, and the total voltage is read on a voltmeter, V_1. A switch, Sw_{14}, is used to reverse polarity. The electron current collected by the focussing anode is measured by a micro-ammeter, A_3. An additional switch, Sw_6, is used to apply voltage directly to the anode.

(c) Analyzer:

A parallel plate electrostatic analyzer, A, similar to that described by Yarnold and Bolton (24), is used for velocity analysis of the scattered beam of electrons. If the beam enters the analyzer at an angle of 45° to the plates, then the energy of the electrons passing through the exit slit, S_3, of the analyzer is given by

$$E = Vx/2d \qquad (1)$$

where

E = energy of the beam passing through the exit slit

V = potential difference between the two plates, P_1 and P_2

x = distance between entrance and exit slits, S_2 and S_3

d = separation of the two plates, P_1 and P_2

For this case, x = 12.5 cm., d = 6.25 cm., and hence, E should be equal to V. The resolving power is given by

$$E/\delta E = x/s \qquad (2)$$

where s, the effective slit width, is equal to the actual slit width minus the thickness of the metal plate in the region of the slit. Using a value of 0.005 cm. for the effective slit width, we obtain a resolving power of about 2500. For an electron beam with an energy of 500 volts, this corresponds to a resolution of two excitations separated by 0.2 volt. The actual performance of the analyzer will be dealt with in a later section. An additional feature of this type of analyzer is the property of image refocussing, whereby electrons of the same energy entering slit S_2 from slightly different directions are focussed on the exit slit, S_3, as shown in Figure 1.

The same battery pack, B_1, is used for applying both accelerating and analyzer voltages. The additional accelerating voltage battery, B_3, is compensated for by a battery, B_5, connected across a fifteen turn Helipot, R_1. The energy difference between incident and scattered electrons is thus measured directly by varying the voltage taken off this

potentiometer.

This arrangement is advantageous in that any drift in voltage of battery, B_1, is common to both accelerating voltage and analyzer circuits, and hence changes in the Helipot reading for a given energy loss are minimized.

Coarse and accurate determinations of analyzer voltages are obtained in a manner similar to that described for the accelerating voltages. In the potentiometric measurement of analyzer voltage, however, Switch Sw_3 must be in the direct position to provide a ground return to the battery from the series resistors, R_{11} and R_{12}. A switch, Sw_8, is used to ground the negative plate, P_1, when the apparatus is not in use to prevent any accumulation of charge.

(d) Electron Multiplier

The electron multiplier, based on a design of J. S. Allen (25), consists primarily of twelve Beryllium-Copper electrodes with good secondary emission characteristics. The incident electron enters through slit, S_5, cut in the electrical shield surrounding the first few electrodes, and strikes the first electrode, releasing several secondaries which are attracted by a potential difference of about 500 volts to the next electrode. This cascade process continues until,

for each incident electron, approximately 10^6 reach the two fine wires of the collector grid, c.g. forming a pulse which is amplified by the pre-amplifier and linear amplifier and counted on the multiscaler. We are indebted to Professor C. H. Shaw, of the Physics Department, for supplying the dynode system.

Since the counting efficiency depends on the energy of the incident electrons, it is desirable to incorporate in the apparatus a means of accelerating or decelerating the incoming electrons. To accomplish this, a battery pack, B_6, is connected across a potentiometer, R_2, and the voltage between the movable arm of the potentiometer and ground is impressed on the slit, S_5. A switch, Sw_{19}, is used to reverse polarity, and a voltmeter, V_2, to measure the impressed slit bias. Figure 4, obtained in the early developmental work, shows the effect of incident electron energy on the counting rate.

A series of resistors, R_{14} - R_{25}, mounted inside the casing under vacuum, are used as a voltage dividing network to give the required 500 volts per stage. The power supply used is a Du Mont Type 263B high voltage power supply with additional filtering action provided by a resistance-capacitance filter, R_{13} - C_1. A microammeter, A_5, measures the current

through, and, therefore, the voltage across, the series of resistors, R_{13} - R_{25}.

(e) Beam Current:

Beam current is defined as that portion of the emitted current which has passed through the final electrode of the electron gun and is eventually collected on some part of the apparatus. This portion of the emission constitutes the beam which is scattered by the gas. In order to measure the beam current, the relay rack housing the control circuits for the electron gun is electrically isolated from the apparatus except for a single ground wire going through the galvanometer, G, before reaching the relay rack. In this way, any leakage currents in the control circuits are not measured as beam current.

(f) Helmholtz Coils:

To obtain reliable results, the forces acting on the electron beam must be only those introduced in the electron gun and analyzer. To accomplish this, the earth's magnetic field is neutralized by two pairs of Helmholtz Coils. The coils used were manufactured by the National Electric Coil Company, of Columbus, Ohio, and consists of 250 turns of number 18 copper wire. One pair of coils has a radius of 30 inches, the other pair, a radius of 32 inches. The cross section is a rectangle approximately 1" x 1/2".

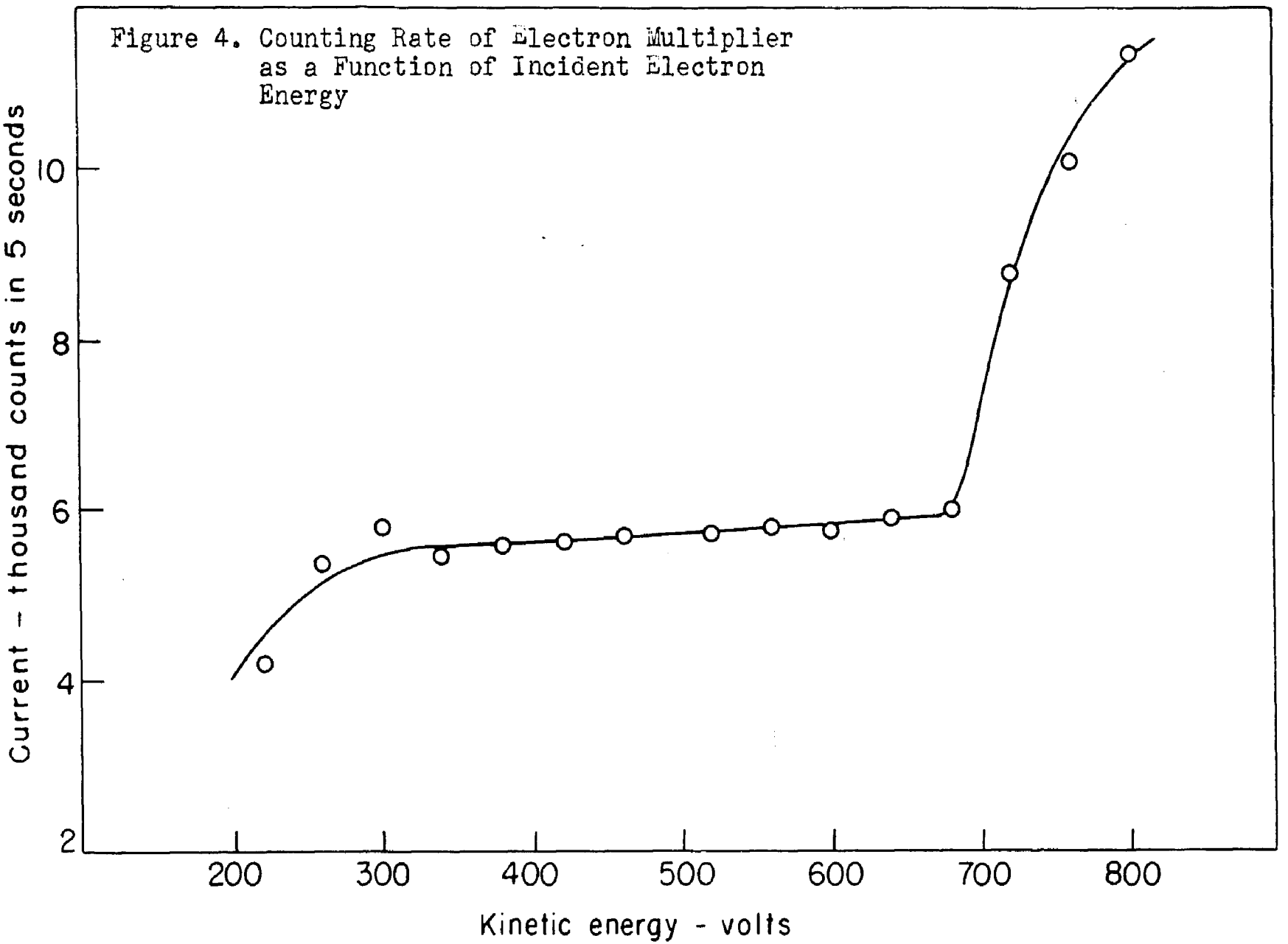

Figure 4. Counting Rate of Electron Multiplier as a Function of Incident Electron Energy

A rotating coil magnetometer, similar to that described by Berman (21), designed by Mr. Homer Weed, is used as a measure of the residual magnetic field. The induced e.m.f. of the rotating coil is amplified by a G. E. phono amplifier and viewed on a Du Mont Type 304-H oscilloscope. The current through the coils is then adjusted for a minimum induced e.m.f. Typical currents used are 45 milliamperes in the vertical and 128 milliamperes in the horizontal coils.

(g) Auxiliary Electronic Equipment

An Atomic Instrument Company Model 206A preamplifier is used as an impedance matching device between the electron multiplier and an Atomic Instruments Company Model 204B fast linear amplifier similar to that described by Jordan and Bell (26). An Atomic Instruments Company Model 106 Multiscaler is used for measuring the number of counts. The monitoring oscilloscope is a Du Mont Type 303 suitable for use with high speed pulses.

The measured number of counts during the ten second time interval used during this investigation shows a maximum scatter of ten percent and an average of four percent. This has been traced in part to the twenty minute timing clock in the multiscaler. A greater accuracy of measurement could be obtained by replacing this timer by a two minute clock.

A discriminator circuit is included in the multiscaler by means of which pulses below a chosen amplitude may be rejected before reaching the counting circuits. Experience has shown that a discriminator voltage of about two volts is sufficient to exclude power supply ripple and amplifier noise and allow pulses from the electron multiplier to pass.

(h) Miscellaneous

For reference purposes, a number of important dimensions will be given in this section. The radius of the collision chamber is 9.41 cm. The distance from the center of the collision chamber to the coarse slit, S_1, is 8.04 cm., and from the center to the last electrode of the electron gun, is 2.54 cm. The distance from the coarse slit, S_1, to the fine slit, S_2, is 11.43 cm., and from the fine slit, S_3, to the coarse slit, S_4, is 17.75 cm. The total path length of the beam from the electron gun to the analyzer is thus 22.0 cm. The slit dimensions are summarized in Table 2. The widths of the fine slits could not be measured accurately and the values given are therefore only approximate.

Brass is used throughout the construction of the apparatus with the exception of the base plate of the multiplier casing. This is made of lucite sheet to prevent leakage or breakdown from the high voltage input to the casing.

Table 2

Slit Dimensions

	Width (cm.)	Length (cm.)
Collision Chamber-Analyzer:		
Coarse Slit, S_1	0.093	1.05
Fine Slit, S_2	0.005	0.915
Analyzer-Electron Multiplier:		
Coarse Slit, S_4	0.192	1.015
Fine Slit, S_3	0.005	0.905

B. Operation and Performance of the Spectrometer.

Two types of measurements are ordinarily made with the electron spectrometer: (1) spectra of the energy losses suffered by the incident electron beam during its passage through the gas, and (2) measurements of the variation of scattered current with angle for a definite atomic or molecular transition.

Energy spectra are obtained by setting the electron gun at a fixed angle and reading the number of counts in a given time interval for different readings of the Helipot, R_1, over the voltage range of interest. Figure 5 shows an energy spectrum for helium obtained during the early developmental work on the apparatus. The first three transitions of helium at 21.22, 23.09, and 23.74 volts are clearly evident here. The spectrum of nitrogen, with the most prominent transition at 12.9 volts, is also present even though the residual pressure was less than 1×10^{-5} mm. Hg. An additional impurity, presumed to be hydrocarbons from the pump oil, gives energy losses in the region around 6 volts. After several hours of pumping, the intensity of this background scattering of nitrogen is reduced to about 4 percent of the $1^1S - 2^1P$ peak of helium, and after several weeks to about 2 percent, and is therefore negligible. Vacuum spectra

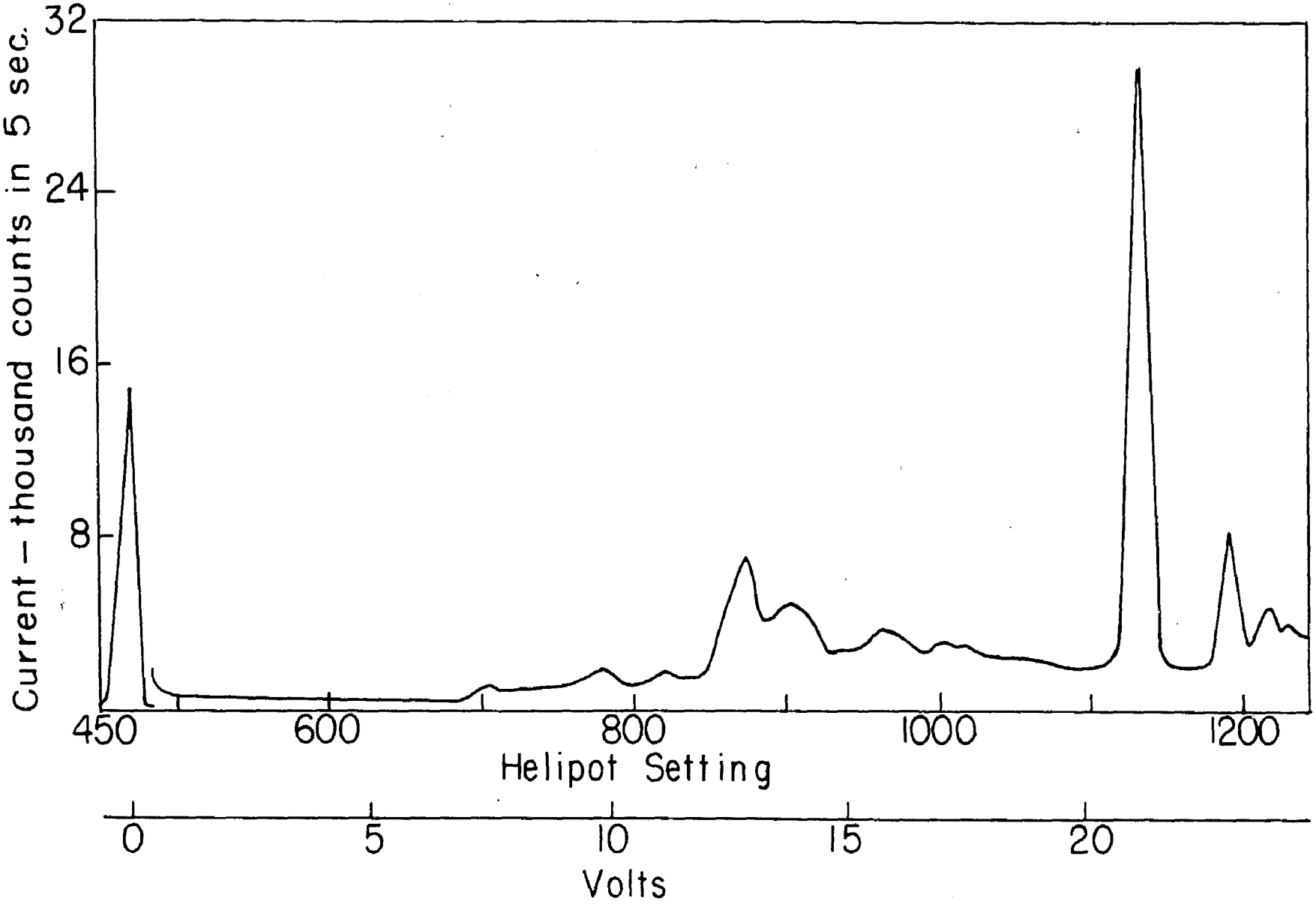

Figure 5. Energy Spectrum of Helium

are, however, taken at periodic intervals during an investigation to insure that the background remains insignificant.

The energy loss of a given excitation is determined from the equation

$$W = k\ D\ E_o\ /\ 1500 \qquad (3)$$

where

k = a constant dependent on the characteristics of the analyzer

D = the number of divisions on the 1500 division Helipot, R_1, between the direct beam (i.e., those electrons with no energy loss) and the excitation under consideration

E_o = the voltage of the fine analyzer battery, B_5

W = energy loss for the excitation under consideration

The 1^1S - 2^1P transition of helium at 21.22 volts may be used to determine the constant k. For this work, sixteen runs on helium were used, giving $k = 1.01_9$ which may be compared with the theoretical value of 1.000 obtained from equation (1).

Angular scattering runs are made by taking current readings for several settings of the Helipot, R_1, in the neighborhood of the peak to insure obtaining the maximum current reading for the transition under study. This procedure is carried out for several angles on both the positive and negative sides of the zero angle. The gun is always rotated in the

same direction during the course of a run to avoid any errors due to backlash in the worm gears. The readings are then plotted with current as ordinate and gun angle as abscissa and the zero angle is determined from the symmetry of the curve. For a given scattering angle the currents are then read from the smooth curves on both the positive and negative sides and the average taken as the current reading for that angle. Two or more runs are made for each set of conditions and the current averages for all runs are then averaged. These final data are the ones used for the calculations mentioned in subsequent sections. An example of these calculations is given by Table 3, listing the raw data, Figure 6 showing the smooth curves, and Table 4 giving the currents at positive and negative angles and their averages. These data are for the 8.35 volt excitation potential of carbon monoxide with an accelerating voltage of 508.8 volts, a beam current of 3.14 microamperes and a gas pressure of 4.9×10^{-4} mm. Hg.

The scattered current sensitivity may be seen from Table 3. The lowest current used was about 200 counts in 10 seconds, corresponding to approximately 3×10^{-18} amperes.

Table 3

Angular Scattering of the 8.35 Volt Excitation of Carbon Monoxide at 508.8 Volts

Gun Angle-degrees	Counts in 10 sec.	Gun Angle-degrees	Counts in 10 sec.
16	217	-2	90579
15	280	-2.5	60439
14	397	-3	38559
13	587	-3.5	26387
12	948	-4	18780
11	1459	-5	9542
10	2507	-6	5355
9	4193	-7	3437
8	6993	-8	2064
7	11382	-9	1380
6	24399	-10	770
5	56033	-11	561
4.5	78007	-12	358
		-13	264
		-14	194

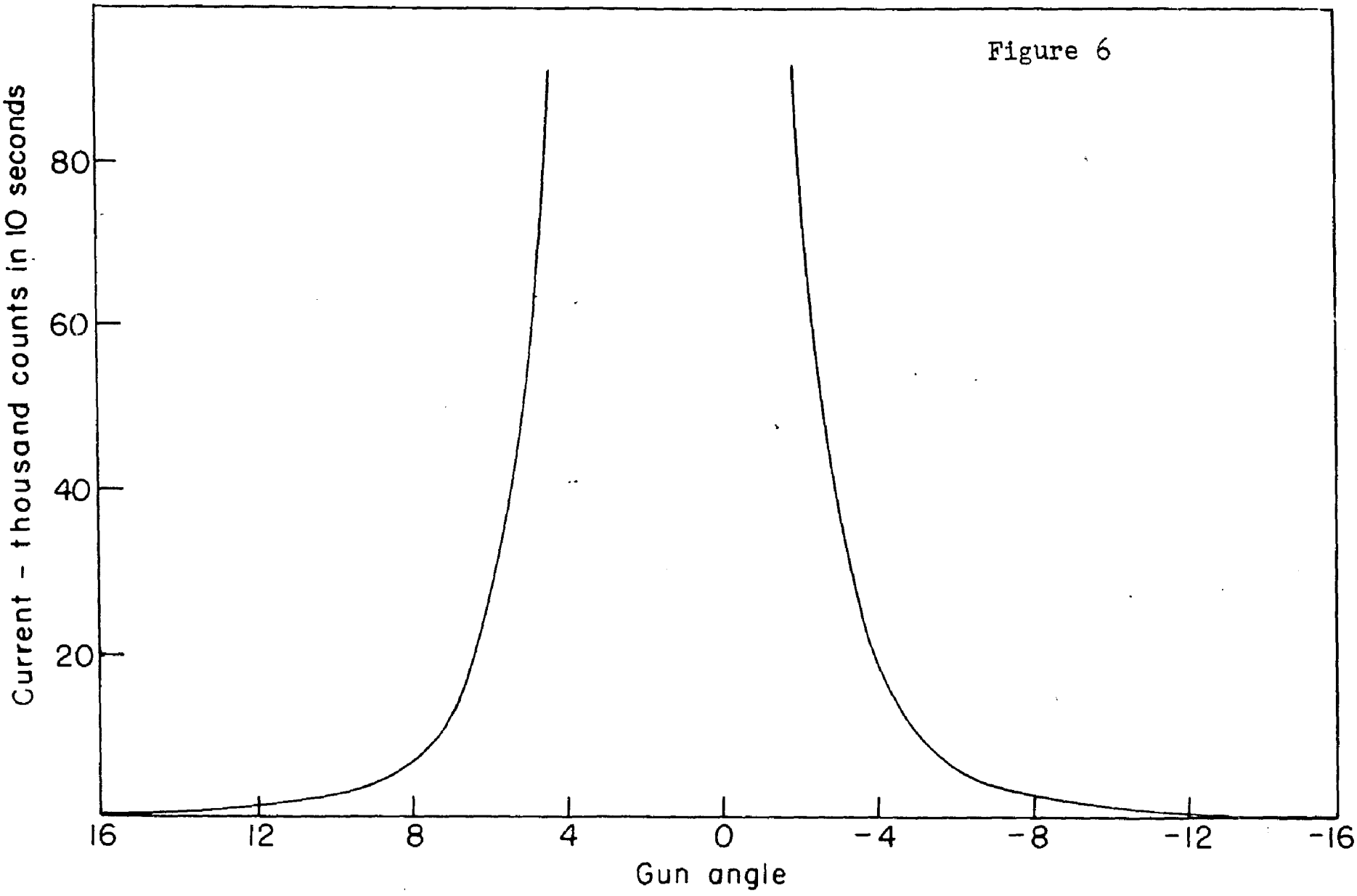

ANGULAR SCATTERING OF THE 8.35 VOLT TRANSITION OF CARBON MONOXIDE AT 508.8 VOLTS

Table 4.

Angular Scattering of 8.35 Volt Excitation of Carbon Monoxide

Zero Angle = 1.20° ± 0.01°

Scattering Angle - Degrees	Pos. Gun Angle - Degrees	Counts in 10 sec.	Neg. Gun Angle - Degrees	Counts in 10 sec.	Average Counts in 10 sec.
3.5	4.7	67200	-2.3	70500	68850
4.0	5.2	46800	-2.8	46300	46500
4.5	5.7	31100	-3.3	31250	31175
5.0	6.2	20750	-3.8	21300	21025
5.5	6.7	14250	-4.3	14800	14525
6.0	7.2	10100	-4.8	10700	10400
6.5	7.7	7750	-5.3	8000	7875
7.0	8.2	6200	-5.8	6000	6100
7.5	8.7	4870	-6.3	4650	4760
8.0	9.2	3720	-6.8	3630	3675
8.5	9.7	2870	-7.3	2900	2885
9.0	10.2	2200	-7.8	2300	2250
9.5	10.7	1700	-8.3	1850	1775
10.0	11.2	1330	-8.8	1450	1390
10.5	11.7	1050	-9.3	1130	1090
11.0	12.2	850	-9.8	900	875
11.5	12.7	680	-10.3	720	700
12.0	13.2	550	-10.8	570	560
12.5	13.7	450	-11.3	470	460
13.0	14.2	370	-11.8	390	380
13.5	14.7	300	-12.3	320	310
14.0	15.2	250	-12.8	270	260
14.5	15.7	220	-13.3	230	225
15.0	16.2	180	-13.8	190	185

The increased resolving power of the new apparatus is vividly illustrated by Figure 7 which shows a portion of the helium energy spectrum at 235 volts and a scattering angle of 9^{o}. The optically forbidden transition, $1^{1}S - 2^{1}S$, is clearly evident here and is also found at wide angles at energies up to at least 600 volts. This transition has previously been observed, by Womer (27), for energies of the incident beam lower than 70 volts.

The half-width of a peak for incident electron energies of 500 volts is of the order of 0.4 volt. Of this, approximately 0.2 volt is due to the analyzer (cf. equation 2), and 0.2 volt to the thermal energy spread of the beam leaving the emitter.

One of the problems that arose during the development work was that of obtaining a well collimated electron beam. Theory indicates that a potential difference between focussing anode and cathode of either four times or one-fourth the accelerating voltage will focus the beam. A high positive (with respect to ground) focussing voltage was tried, but this proved impracticable because of the gas discharge in the gun and breakdowns between electrodes. The use of

Figure 7.

HELIUM SPECTRUM AT 235 VOLTS AND SCATTERING ANGLE 9°

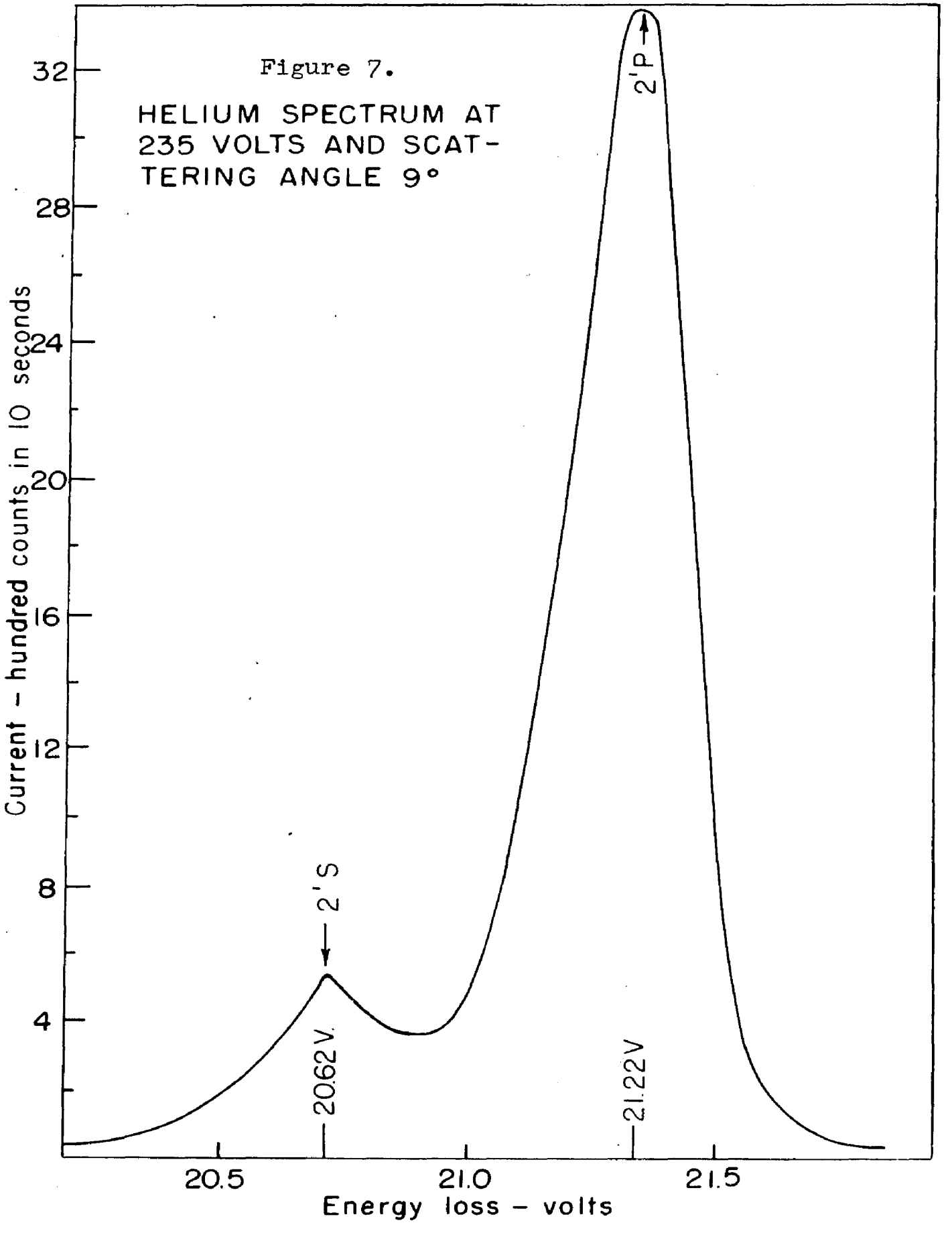

a negative focussing voltage, however, was successful. Figure 8 shows the difference in the shape of the angular scattering curve with and without a focussing voltage. The data used are from runs made on April 7, 1952, on the $1^1S - 2^1P$ transition of helium at an accelerating voltage of 500 volts, a beam current of 0.157 microamperes, and a gas pressure of 4.9×10^{-5} mm. Hg. The method used to determine the optimum focussing voltage is to set the gun angle at the approximate zero angle and adjust the focussing voltage to obtain the maximum current for a given transition, usually the $1^1S - 2^1P$ transition of helium. This technique is illustrated in Figure 9, from data taken on April 23, 1952, where the counting rate is plotted against focussing voltage.

Another matter of some interest is the shape of the direct beam, since from this the angular divergence of the electron beam may be obtained. One method of measuring this is to read the currents in the high voltage microammeter, A_5, as the angle is varied on both sides of the zero angle. Figure 10, from a run made on April 12, 1952, illustrates this procedure and gives a cone angle for the electron beam of about 40 minutes.

In order to obtain accurate measurements of the angular scattering, it is necessary that the collected current be proportional to the incident current. Figure 11, using the

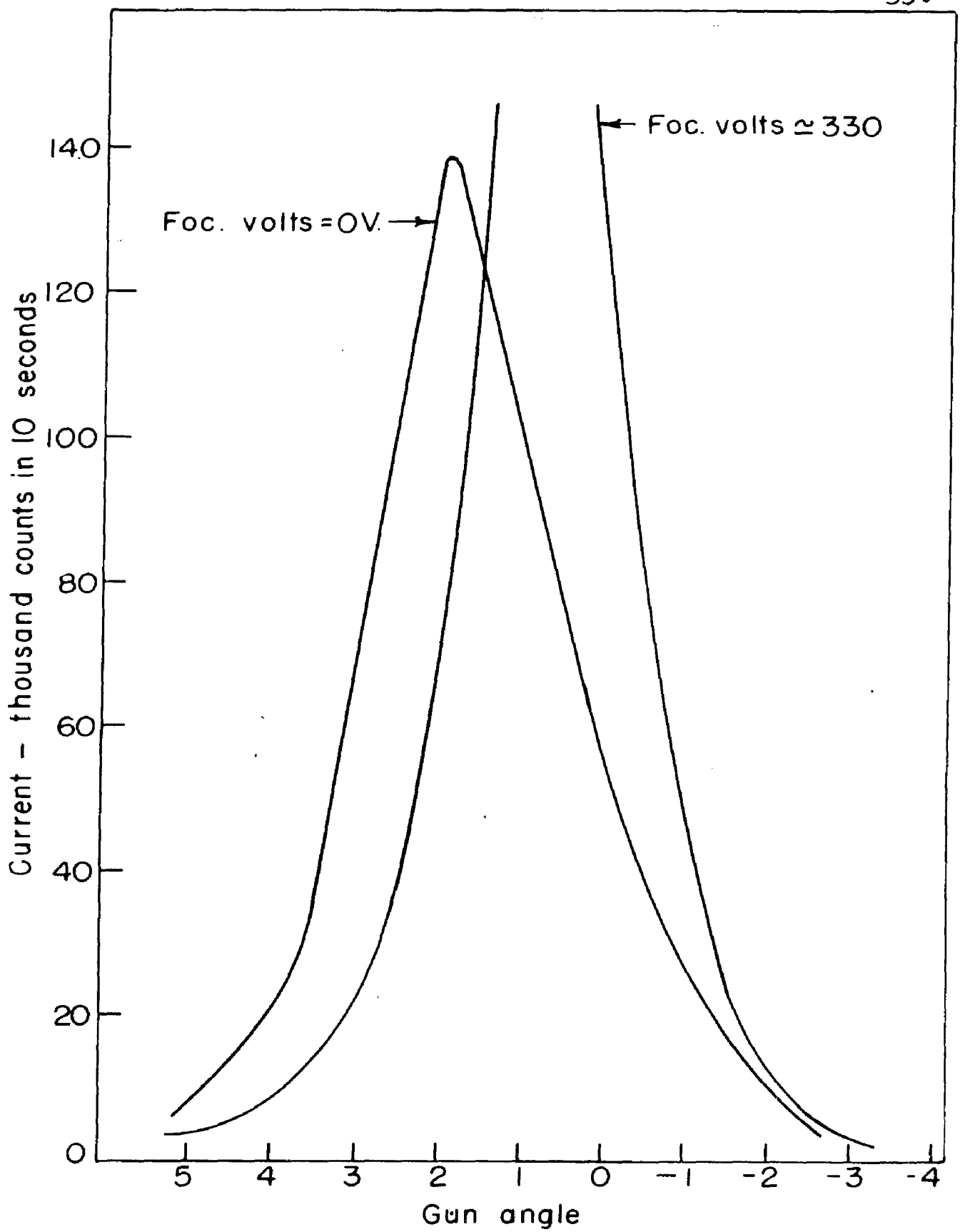

Figure 8. Effect of Focussing Voltage on Beam Shape

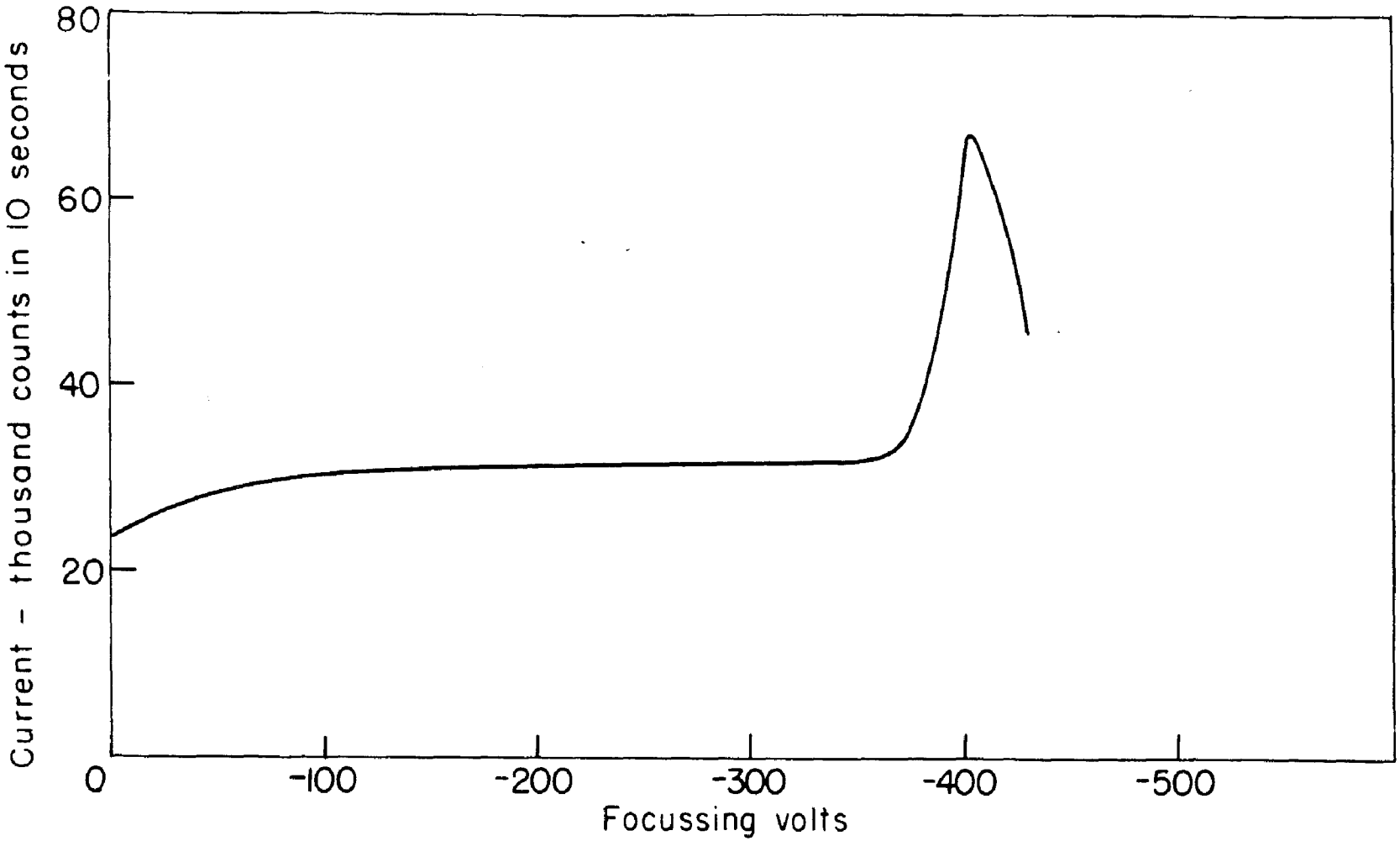

Figure 9. Effect of Focussing Voltage on Counting Rate

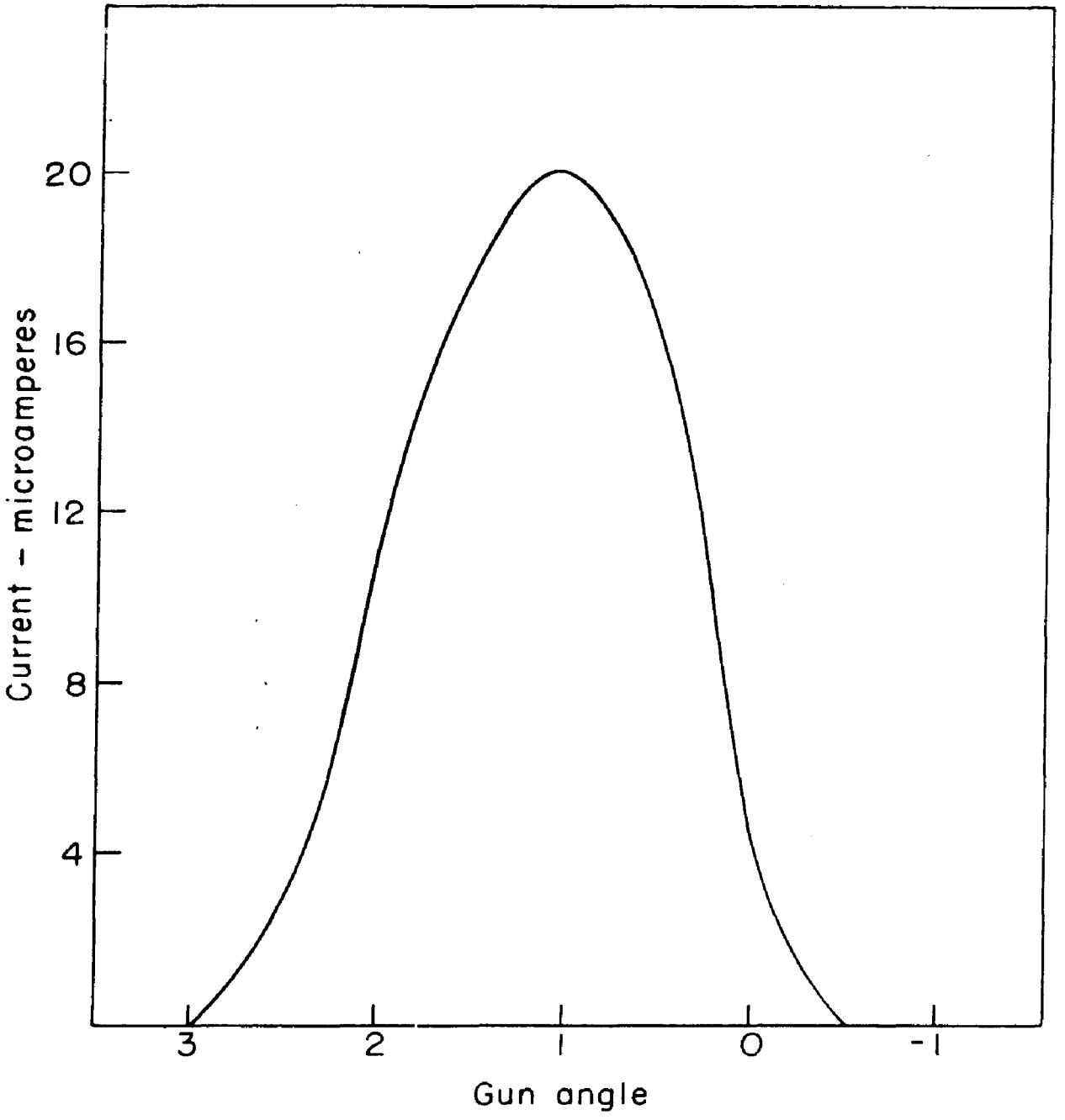

ANGULAR SHAPE OF THE DIRECT BEAM

Figure 10.

data taken on April 17, 1952 shows this proportionality for the $1^1S - 2^1P$ transition of helium.

One further observation concerning the electron gun should be made. It was found that at low beam currents the collected current and the beam direction were extremely unstable. All measurements were therefore carried out at a beam current of 3.14 microamperes. The reason for this behavior is not clearly understood at the present time, although all indications are that the oxide-coated emitter is responsible. It is hoped that further work on the electron gun to remove these undesirable features will be carried on in the future.

C. Presentation of Data

Francis (17) and Jones (18) have shown that cross sections for atomic scattering substances may be obtained from the equation

$$\sigma_i = \frac{K'be^{\alpha pl}}{PV(E-W_i)} \frac{I}{I_o} \qquad (4)$$

where

- K = an apparatus constant determined by calibration with helium
- b = $\int i dW / I$ = ratio of area to height for the transition under study. Here i = scattered current for a given energy loss W
- I = peak current for the transition under study
- α = total absorption coefficient
- P = pressure of the gas in the collision chamber
- l = path length of the electron beam through the scattering gas
- V = scattering volume
- E = energy of the incident electrons
- W_i = energy loss for the transition under consideration
- I_o = beam current

For molecular scattering substances, the molecular excitation cross section per unit energy range, S_i, is given by

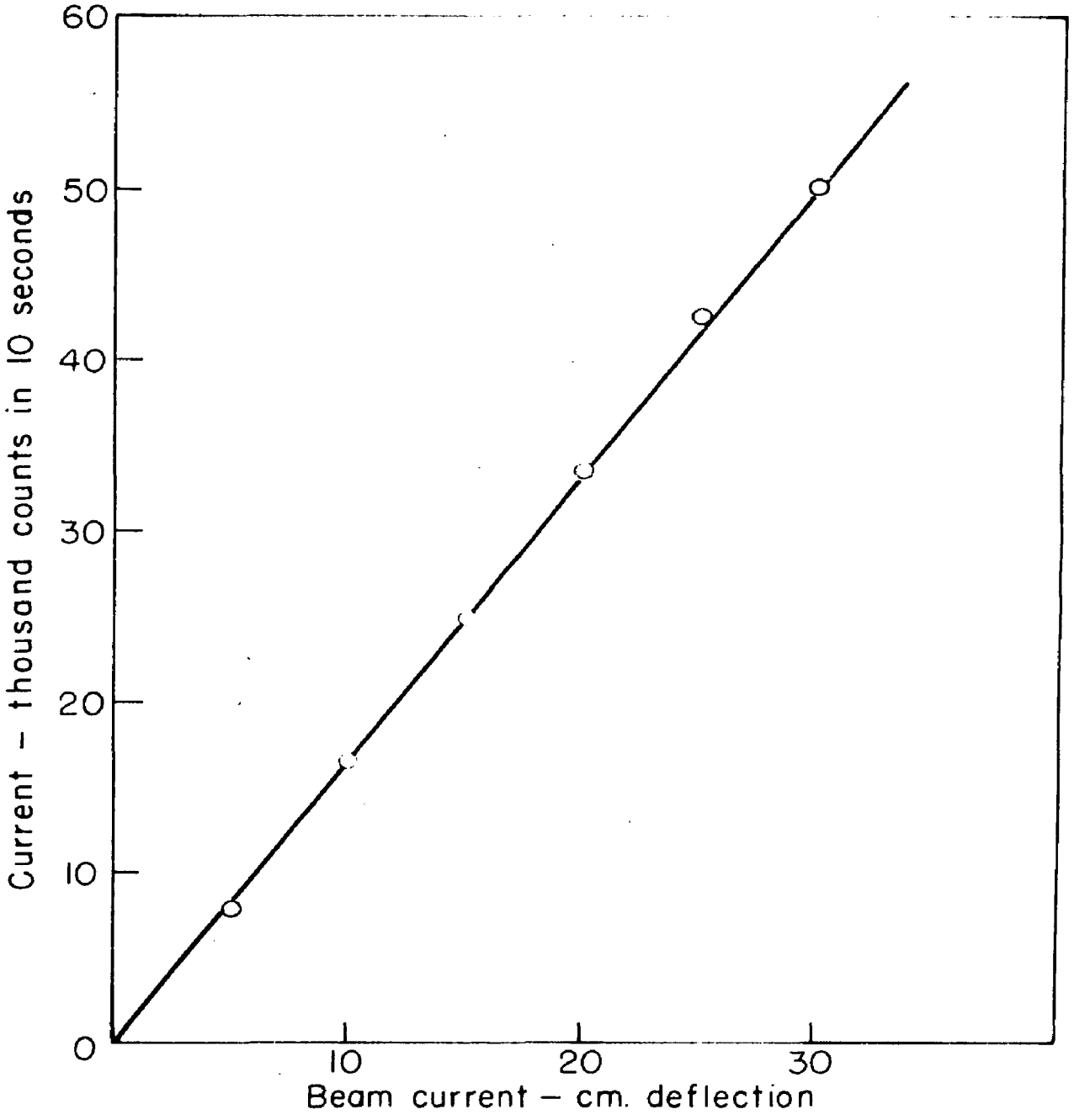

PROPORTIONALITY OF COLLECTED CURRENT TO BEAM CURRENT

Figure 11.

$$S_i = \frac{K' e^{\alpha p l}}{PV (E-W_i)} \quad \frac{I}{I_o} \qquad (5)$$

an expression identical with equation (4) except for the factor b. The symbols here have the same meaning as in equation (4). At the scattering angles, θ, used in this work, the scattering volume, V, is inversely proportional to sin θ. In addition, the beam current was 3.14 microamperes during the entire study. Hence, these constant factors and all conversion factors may be incorporated in the apparatus constant, K', to give an expression for the cross sections in terms of directly measured quantities. We have, then,

$$S_i = \frac{K e^{\alpha p l}}{P (E-W_i)} \quad I \sin \theta \qquad (6)$$

where

P = pressure in mm. Hg.

l = path length in cm.

E, W_i = energies in volts

I = current as counts in 10 seconds

The apparatus constant, K, used in this work was determined by averaging the currents for fourteen runs on the angular

scattering of the $1^1S - 2^1P$ transition of helium. Theoretical values of the cross sections, σ_i, and of the quantity $\sigma_i \frac{Pm}{Pn} \Delta p^2$ are given by Jones (18). The details of this calculation are given in table 5. Four runs on the area of this transition were used to obtain a b-value of 0.505.

Table 5

Determination of Apparatus Constant

E = 511.28 volts W = 21.22 volts

θ	ΔP^2	Average Counts in 10 sec.	(exp.) $\frac{\sigma i}{Kb} \frac{Pm}{Pn} \Delta P^2$	(theor.) $\sigma_i \frac{Pm}{Pn} \Delta P^2$	Kb
4.5	0.2447	35063	2834.6	0.477	1.682×10^{-4}
5.0	0.2983	23816	2607.3	0.440	1.688×10^{-4}
5.5	0.3573	16380	2362.1	0.404	1.710×10^{-4}
6.0	0.4220	11800	2191.8	0.373	1.702×10^{-4}

Average Kb = 1.696×10^{-4}

b = 0.505

K = 3.358×10^{-4}

Examples of this calibration procedure are given in much greater detail in the theses of John (20) and Edmisten (22).

Another quantity of interest is the square of the change in momentum on impact. This has been given by Francis (17) and Berman (21) as

$$\Delta P^2 = 8 \bar{E} \left[\sin^2 \frac{\theta}{2} + (W/4\bar{E})^2 \right] \qquad (7)$$

where

$$\bar{E} = (E + (E - W)) / 2 = E - \frac{W}{2}$$ and is in atomic units.

The quantity $W/4\bar{E}$ is dimensionless and W and $\bar{E}$ should be in the same units for this calculation.

If the logarithmof equation (4) is taken, we obtain

$$\log (I/P) = \log \frac{\sigma_i V (E - W_i) I_o}{K'b} - \frac{\alpha p l}{2.303} \qquad (8)$$

Thus from the slope of a plot of log (I/P) against pressure for a given accelerating voltage and scattering angle a value at α 1 and hence α may be determined. Figure 12 is an example of such a plot for carbon monoxide at an accelerating voltage of 500 volts and scattering angle of 6° , and Table 6 gives the values of α used in this work. These values are about three times higher than those given by Normand (9).

Table 6

Absorption Coefficients for Carbon Monoxide

Voltage	α
420	51
500	40
600	37

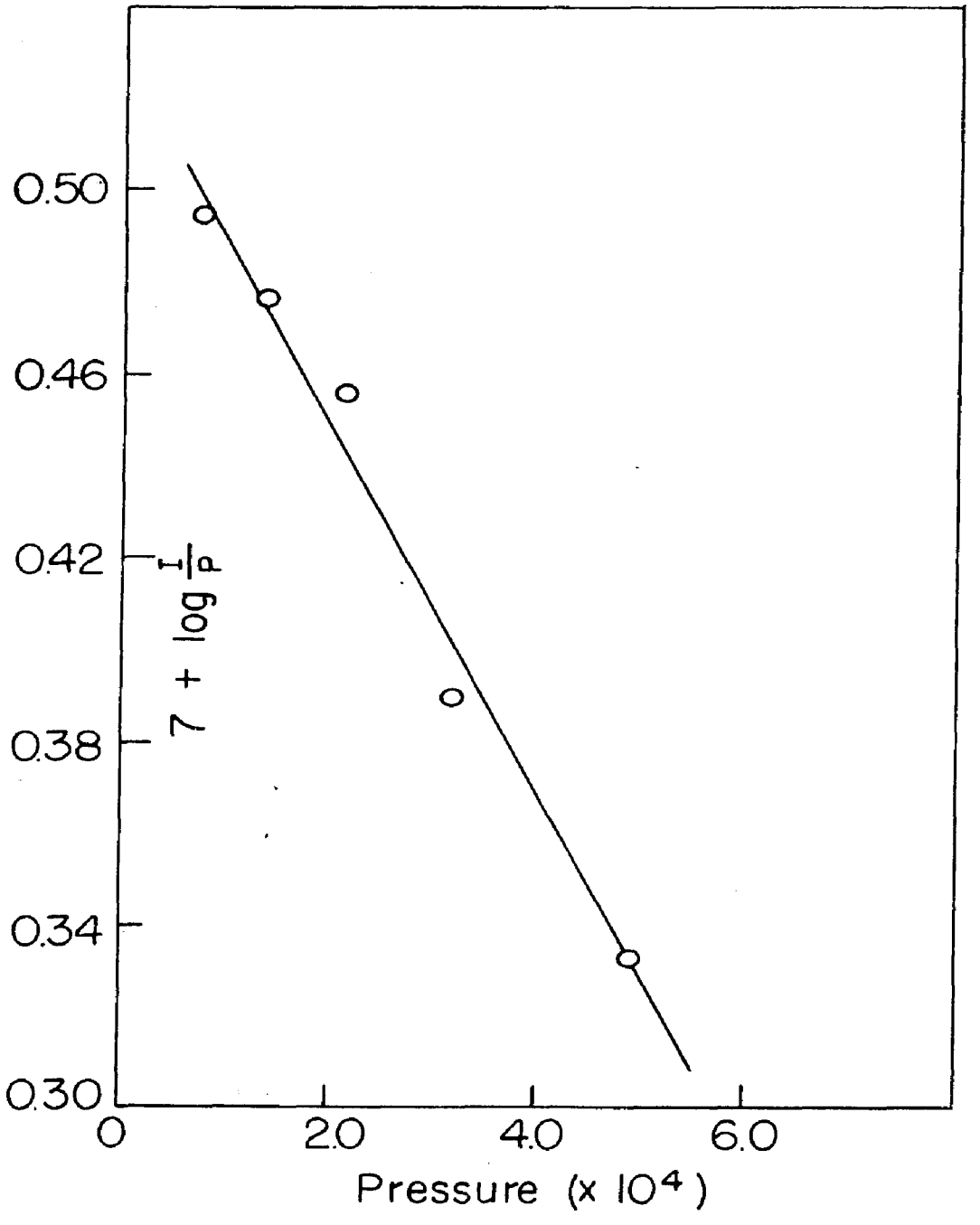

Figure 12. Determination of Absorption Coefficient

This phenomenon has also been noted for all gases which have been studied by all previous workers in this laboratory, using another apparatus and several different types of pressure gauges. The reason for this behavior is not yet completely understood. Normand's work is open to some criticism at these voltages because of the low resolving power of his apparatus. In addition, the electron spectrometer is not ideal for measuring total absorption coefficients, since errors in the counting rate and pressure measurement have an important effect on the numerical value of α. In any event, the values of α, or, more exactly, αl, obtained here are suitable for the experimental conditions actually existent in the electron spectrometer and it is felt that the cross section determinations are reliable. In addition, it should be noted that a large error in the value of α causes a much smaller error in the value of the cross sections.

D. Chemicals

Carbon monoxide was prepared by the action of concentrated sulfuric acid on C.P. formic acid in vacuum and passed through two liquid nitrogen traps. A mass spectrometric analysis by Dr. S. Ruven Smith indicated a purity of greater than 99.9 percent.

Methyl Ethyl Ketone was obtained from the Matheson Company.

An indicated purity of 99.4 percent was found from a determination of the melting point, -87.36°, a freezing point given by Dreisbach and Martin (28), and the heat of fusion given by Timmermans (29).

Baker and Adamson C. P. Acetone was used without further purification. An infrared spectrogram gave an indicated purity of greater than 99.5 percent.

The ketones were introduced into the sample flask with a hypodermic needle. The stopcock was then greased, the ketone frozen with liquid nitrogen, and the air pumped out into a vacuum system. The freezing, pumping, and thawing cycle was continued until a thermocouple gauge showed no pressure increase on pumping.

III. Experimental Results

A. Energy Spectra

Energy spectra were obtained at an accelerating voltage of 500 volts for several scattering angles ranging from 9.9 to zero degrees and at voltages varying from 115 volts to 600 volts. Only selected portions of the data collected will be presented in this thesis. Figures 13, 14, and 15, show how the appearance of the spectra varies as the scattering angle is changed at an accelerating voltage of 500 volts. A more quantitative idea of this change can be obtained from Table 7, which gives the ratio of peak currents of the given peak to that of the 8.35 volt excitation for the major excitations at 10.78 volts, 11.41 volts, and the combined peaks at 13.24 and 13.55 volts.

Table 7.

Intensity Ratios Relative to 8.35 Volt Excitation as a Function of Angle

Scattering Angle-degrees	Ratio for Excitation 10.78	11.41	13.4
8.4	0.16	0.25	0.83
7.3	0.15	0.24	0.83
6.3	0.17	0.30	0.99
5.4	0.21	0.55	1.20
4.6	0.21	0.67	1.27
3.4	0.19	1.04	1.42
0	0.11	1.16	1.01

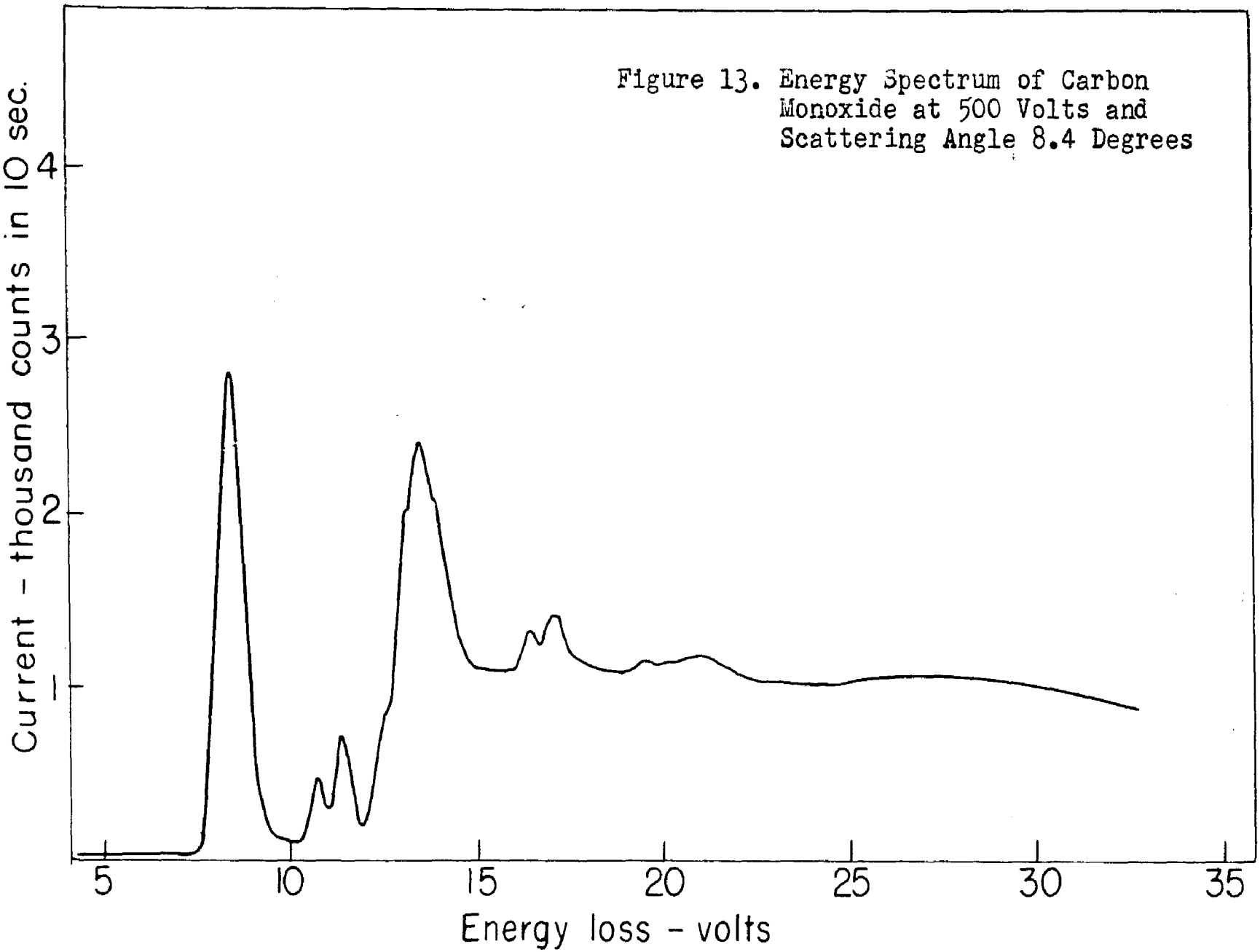

Figure 13. Energy Spectrum of Carbon Monoxide at 500 Volts and Scattering Angle 8.4 Degrees

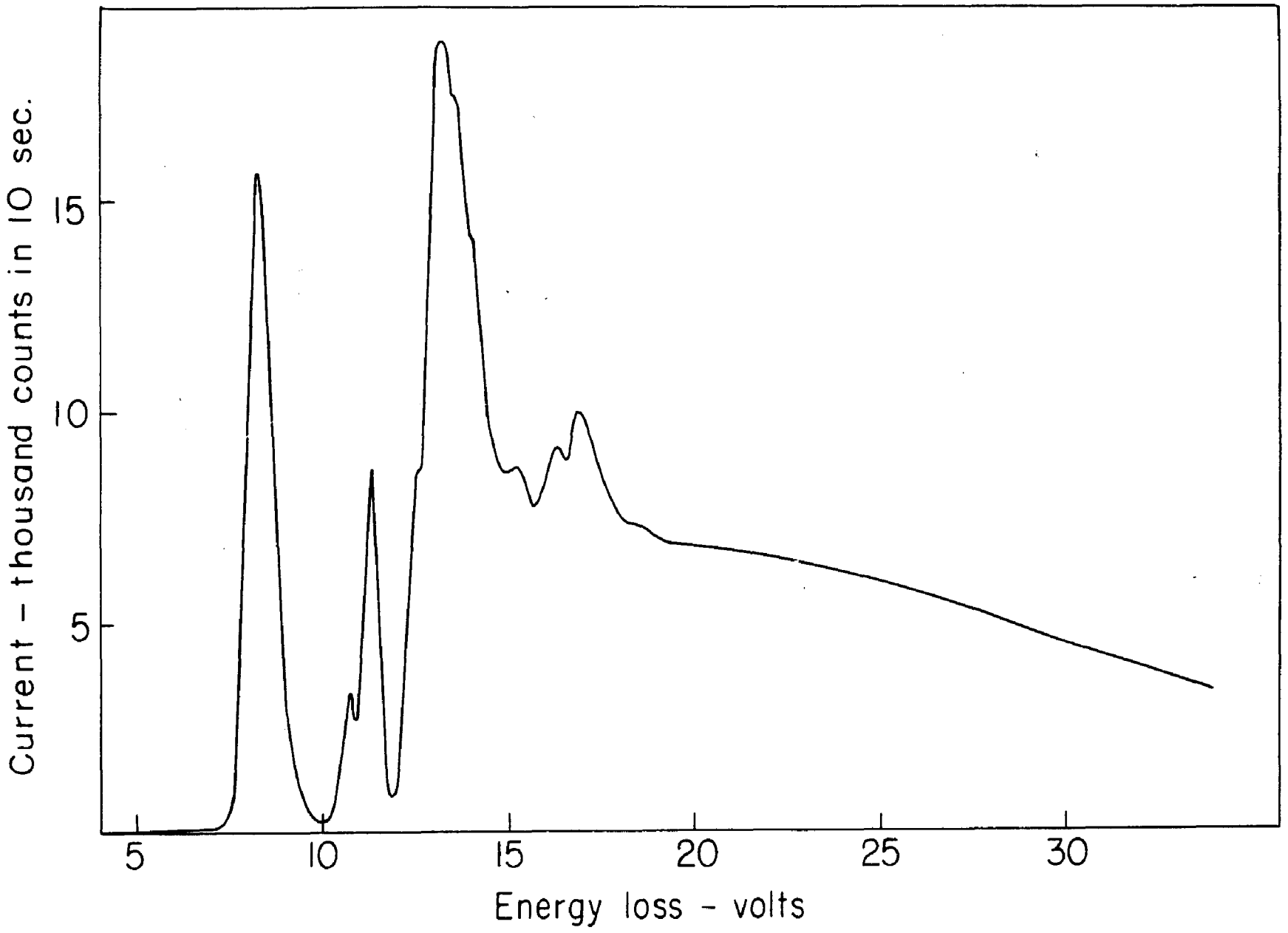

Figure 14. Energy Spectrum of Carbon Monoxide at 500 Volts and Scattering Angle 5.4 Degrees

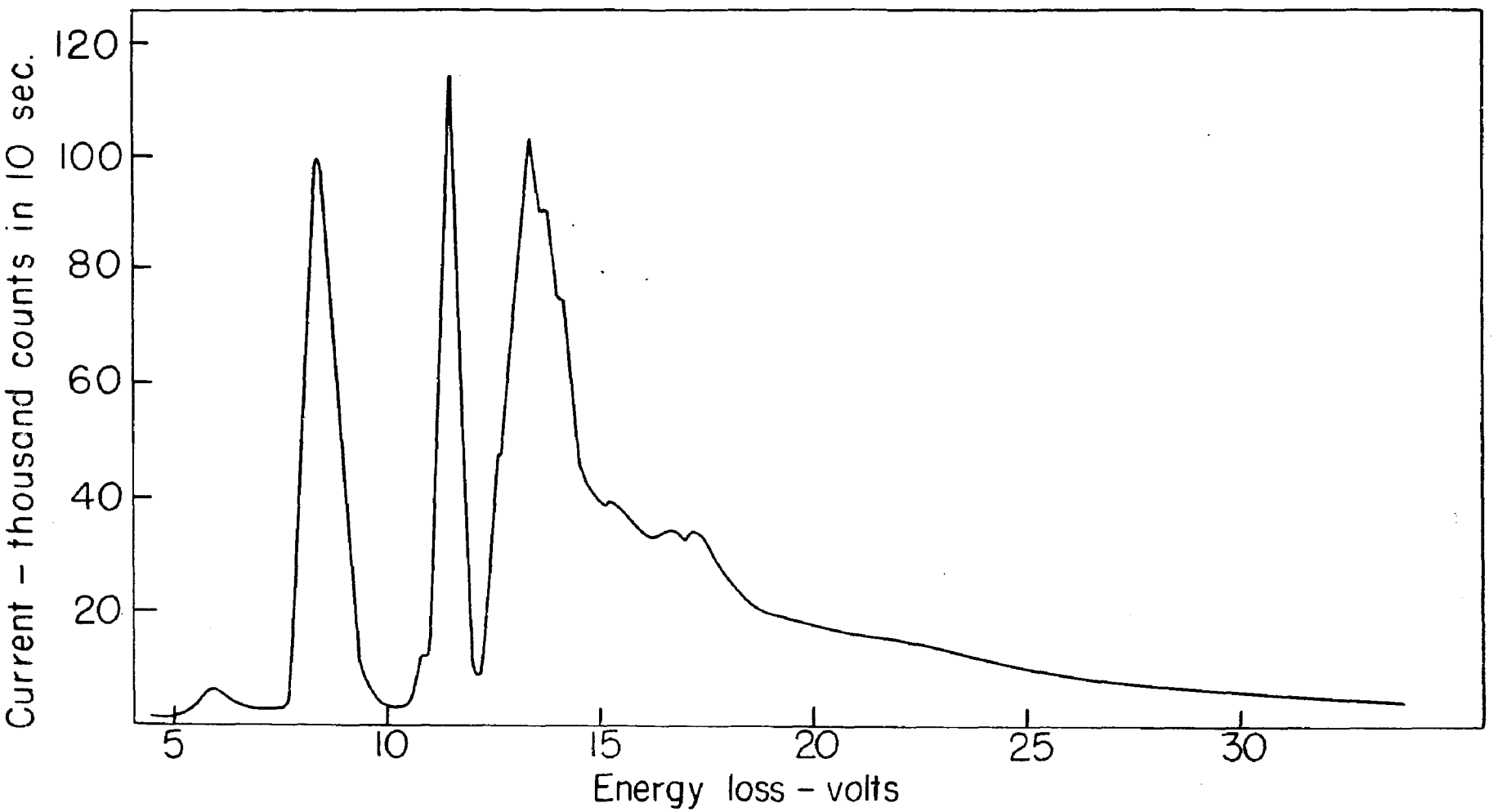

Figure 15. Energy Spectrum of Carbon Monoxide at 500 Volts and Scattering Angle Zero Degrees

The change in appearance of the spectra with voltage is shown in Figure 16, at 500 volts and 3.4 degrees scattering angle; Figure 17, at 325 volts and 2 degrees scattering angle; and Figure 18, at 220 volts and 1.5 degrees scattering angle. Table 8 gives current ratios for the 10.78, 11.41, and the combined 13.24 and 13.55 volt excitations compared with the 8.35 volt excitation at these accelerating voltages. Care must be exercised in interpreting these ratios since the spectrum varies so radically with scattering angle.

Table 8.

Intensity Ratios Relative to 8.35 Volt Excitation as a Function of Accelerating Voltage

Accelerating Voltage	Scattering Angle-degrees	Ratio for Excitation --- 10.78	11.41	13.4
500	3.4	0.19	1.04	1.42
325	2	0.18	1.19	1.01
200	1.5	0.16	1.27	1.14

The excitation potentials determined from well resolved peaks in these spectra occur at 8.35±0.06 volts, 10.78±0.06 volts, 11.41±0.06 volts, 15.24±0.09 volts, 16.46±0.08 volts, and 17.09±0.06 volts. A very broad peak occurs between 12 and 15 volts which is not too well defined. Two excitation potentials which are not always resolved occur with about equal intensity at the maximum of this peak. These are at 13.24

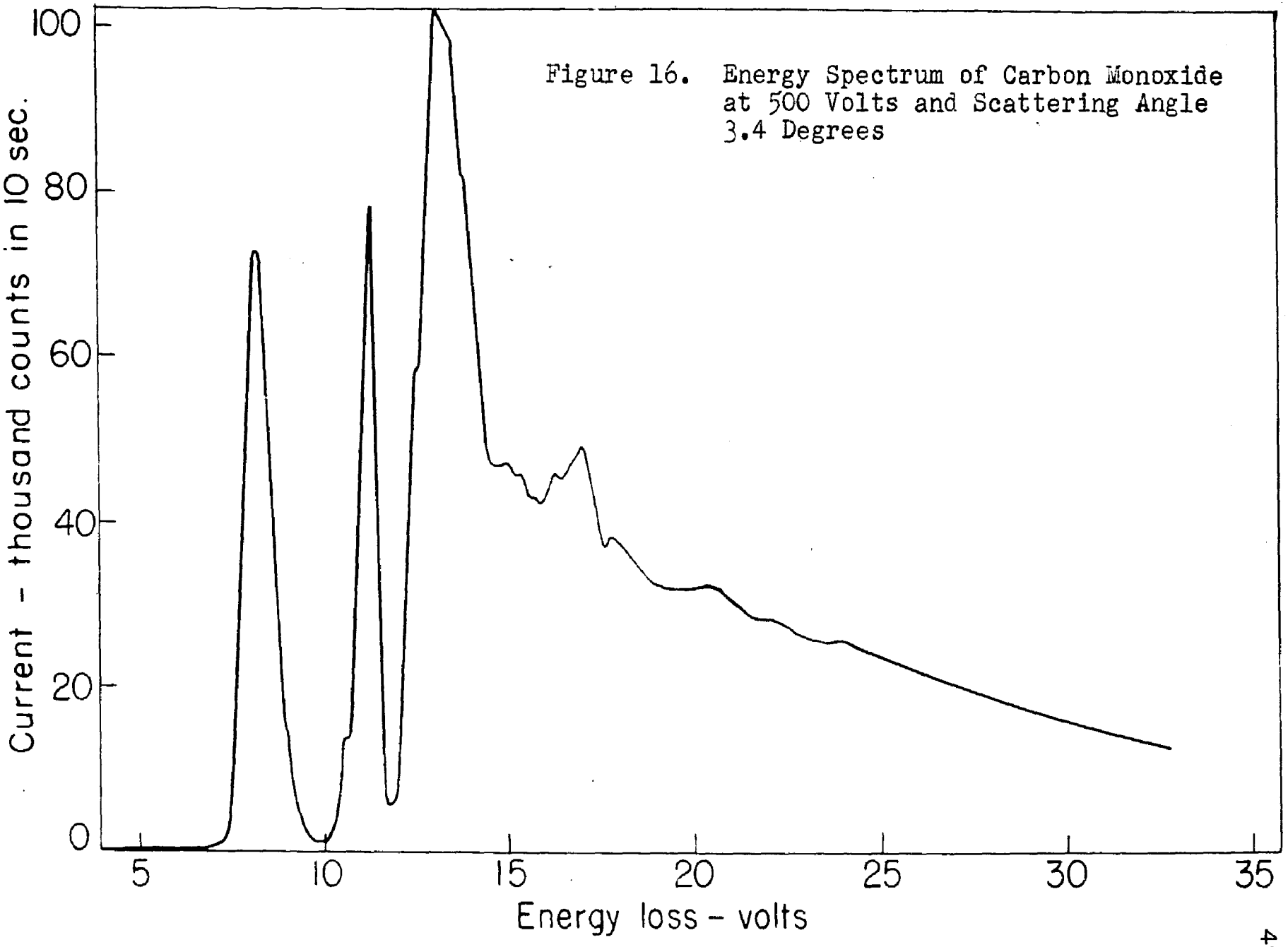

Figure 16. Energy Spectrum of Carbon Monoxide at 500 Volts and Scattering Angle 3.4 Degrees

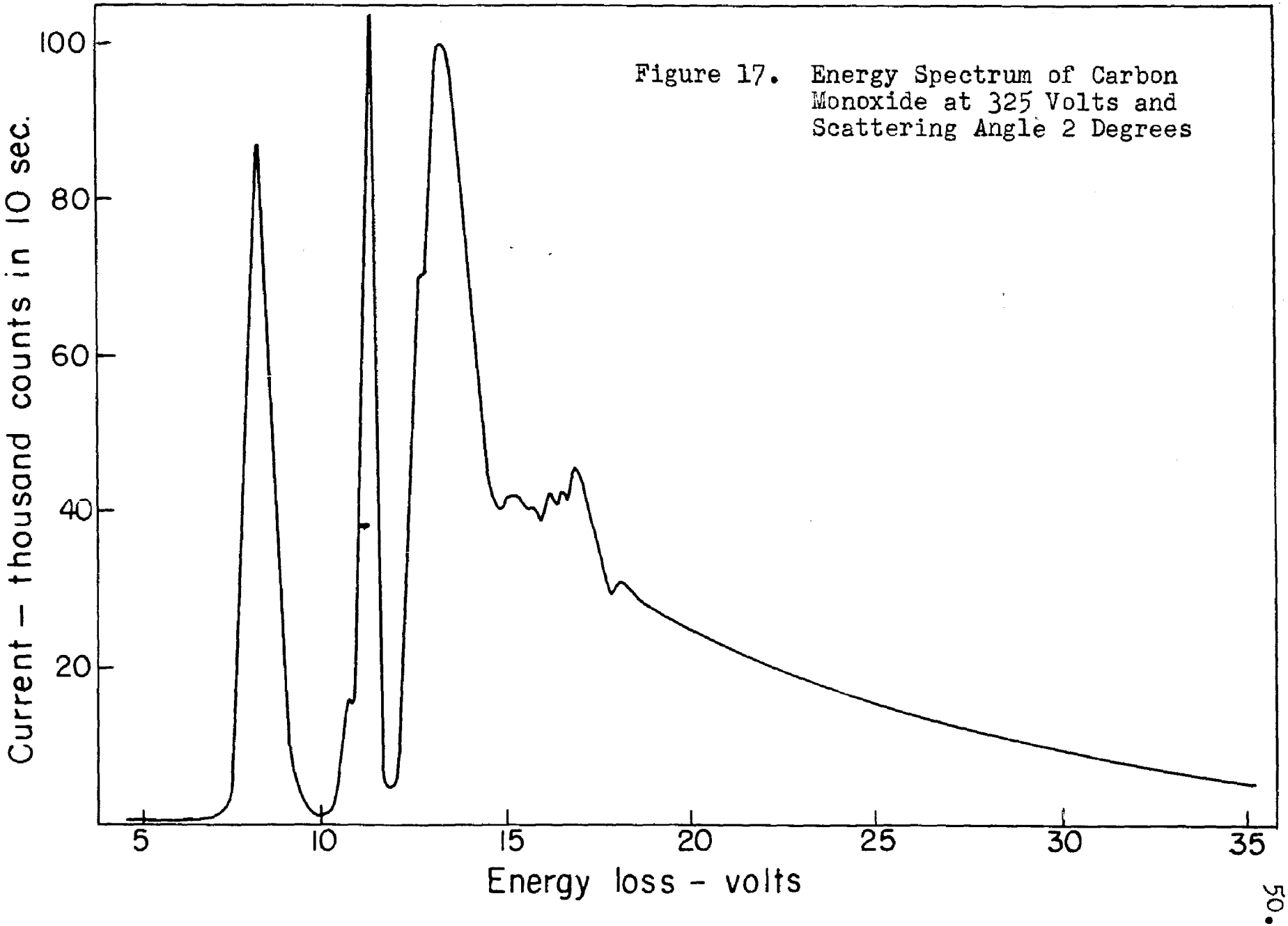

Figure 17. Energy Spectrum of Carbon Monoxide at 325 Volts and Scattering Angle 2 Degrees

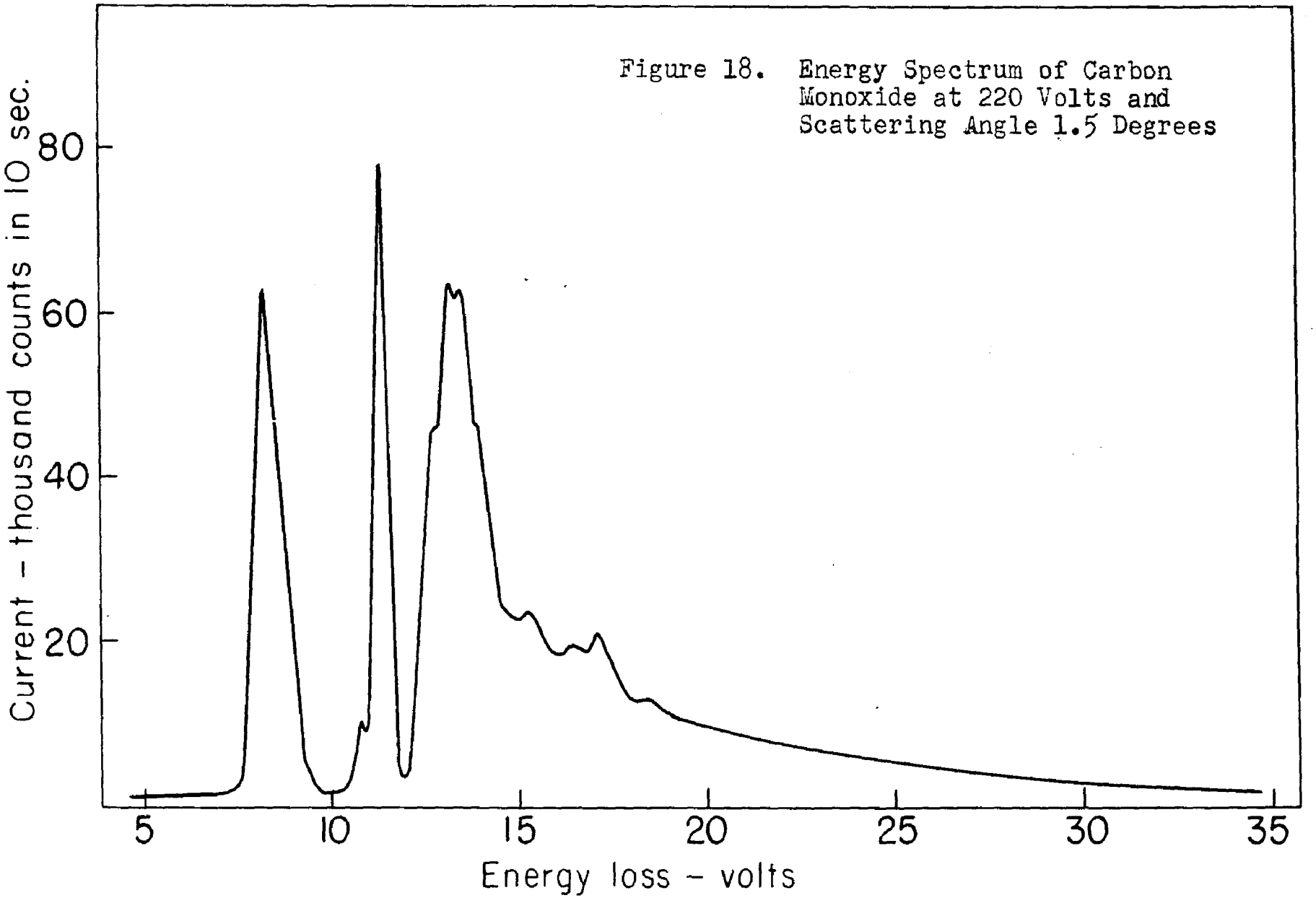

Figure 18. Energy Spectrum of Carbon Monoxide at 220 Volts and Scattering Angle 1.5 Degrees

volts and 13.55 ± 0.06 volts. In addition to these, excitations at 12.57 ± 0.09 volts, 13.87 ± 0.05 volts and 14.24 ± 0.06 volts are apparent as shoulders. The shoulder corresponding to an excitation potential of 12.57 volts occurs at 12.8 volts on the 325 volt spectrum and at 13.0 volts on the 220 volt spectrum, indicating additional unresolved fine structure in this range. An additional feature of the spectra that should be noted is the high intensity over a large range of energy losses of the continuum at wide scattering angles. This effect is also present to a greater extent in the ketone spectra (see Appendix). Table 9 lists the excitation potentials for each run.

Herzberg (30) has given an excellent summary of the spectroscopic work on carbon monoxide. The first excited state, $A^1\pi$, occurs at 8.05 volts, in good agreement with the value of 8.35 volts obtained here when account is taken of the operation of the Franck-Condon principle. The $A^1\pi$ state has an internuclear distance of 1.235 A compared with 1.128 A for the ground state so that the potential energy curve is undoubtedly displaced and excitation to one of the higher vibrational levels would take place. The second and third excited states are both $^1\Sigma^+$ with internuclear distances slightly shorter than in the ground state. These occur at 10.76

Table 9

Excitation Potentials of Carbon Monoxide

Run	Acc. Volts	Scattering Angle	W_1	W_2	W_3
7	500	8.42	8.34	10.79	11.38
8	500	7.32	8.30	10.64	11.35
9	500	6.32	8.37	10.73	11.38
10	500	5.41	8.34	10.79	11.45
1	500	4.58	8.34	10.75	11.34
11	500	3.42	8.40	10.76	11.38
17	500	0	8.44	10.78	11.52
13	325	2°	8.27	10.77	11.36
14	220	1.5°	8.30	10.84	11.39

Run	W_4	W_5	W_6	W_7	W_8
7	12.57	13.19	13.50*	13.81	---
8	12.38	---	13.50*	---	14.28
9	12.54	---	13.62*	---	14.28
10	12.66	13.37*	13.66	---	14.15
1	12.47	13.33	13.60*	13.92	14.28
11	12.63	13.25*	13.53	13.87	14.31
17	12.73	13.10	13.43*	13.77	14.14
13	12.82	13.28*	---	---	---
14	13.03	13.19*	13.53*	13.90	---

Run	W_9	W_{10}	W_{11}	W_{12}
7	---	15.30	16.27	17.11
8	---	15.18	16.39	17.05
9	---	15.33	16.49	17.14
10	---	15.36	16.45	17.02
1	14.67	15.05	16.33	17.10
11	---	15.06	16.52	17.14
17	14.54	15.28	16.58	17.16
13	---	15.32	16.53	16.90
14	---	15.23	16.53	17.12

* indicates maximum scattered current in the 12-15 volt range

and 11.38 volts in excellent agreement with the 10.78 and 11.41 volt excitations determined in this work. In the region above 12.4 volts, a large number of electronic states are present which are not too well defined spectroscopically. In addition, several Rydberg series of bands are present. A quantitative comparison with the electron impact excitations determined here will not be made.

Rudberg (10) studied the energy spectrum of carbon monoxide and found excitations at 8.19, 11.17, 13.24, 16.72, and 21.90 volts, which is in good agreement with the major excitations found here -- except for that at 21.90 volts. Because of the greater resolution of the apparatus used in this investigation, several of the excitations listed by Rudberg were found to be composite. The 11.17 volt excitation, for example, corresponds to the 10.78 and 11.41 volt excitations reported here. No peak was found at 21.90 volts and it is probable that in Rudberg's work this arose from multiple collisions due to the high pressures (7×10^{-3} to 62×10^{-3} mm. Hg.) used.

Finally, it should be noted that the peak at about 6 volts in the zero angle spectrum, Figure 15, is almost certainly due to a hydrocarbon impurity, since the run was made at a pressure of about 1.3×10^{-4} mm. Hg. This peak is also present in the vacuum spectrum.

B. Angular Dependence of the 8.35 Volt Excitation

The angular variation of the scattered current was studied for the 8.35 volt excitation of carbon monoxide at accelerating voltages of 420, 500, and 600 volts with a beam current of 3.14 microamperes and a gas pressure of 4.9×10^{-4} mm. Hg. Tables 10 to 12 list the scattered currents at the various scattering angles for these runs. Using the average current of the two runs at each voltage, there were calculated the molecular cross section per unit energy range, S_i, and the differential oscillator strength. These calculated values are shown in Tables 13 to 15. If the Born approximation is valid, the cross sections, S_i, will be a function of ΔP^2 and will be independent of the accelerating voltage. Figure 19 shows a plot of S_i against ΔP^2 and indicates that the Born approximation is valid down to at least 420 volts.

A quantity of great interest is the generalized oscillator strength, f_i, which has been defined by Bethe (31) as

$$f_i = \frac{2W_i |\varepsilon_i|^2}{\Delta P^2} \qquad (9)$$

where W_i and ΔP^2 are as previously defined, and

$$\varepsilon_i = \sum_s \int \psi_o e^{i \Delta P z_s} \psi_i^* d\tau \qquad (10)$$

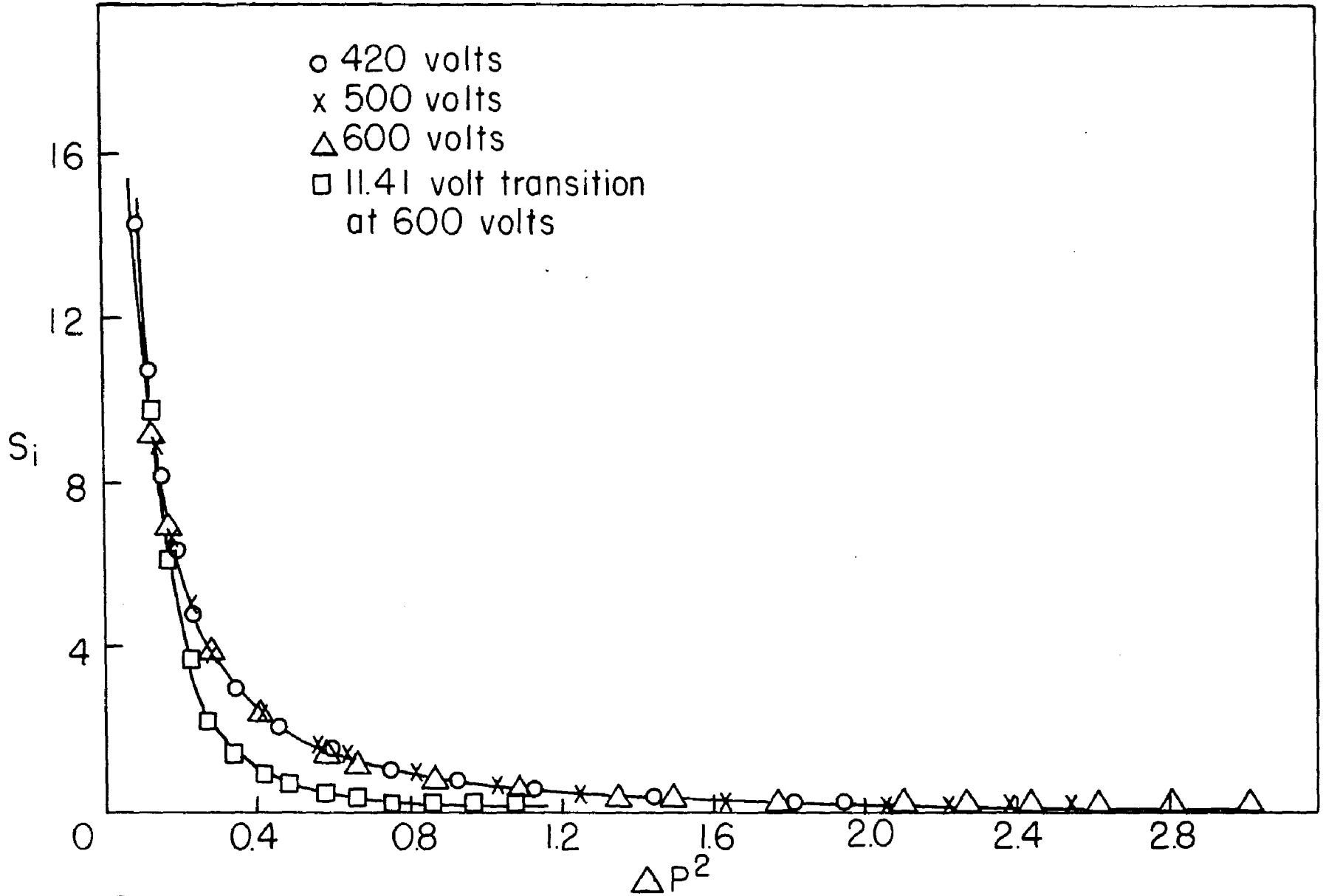

Figure 19. Molecular Cross Sections as a Function of Change of Momentum on Impact

Table 10.

Scattered Currents for the 8.35 Volt Excitation at 420 Volts

E = 415.95 volts, Pressure = 4.9×10^{-4} mm. Hg,

Zero Angle for Run 1 = $1.16^{\circ} \pm 0.02^{\circ}$, Zero Angle for Run 2 = $1.59^{\circ} \pm 0.01^{\circ}$

θ	I Run 1	I Run 2
3.0	96750	90500
3.5	60500	60875
4.0	40600	40500
4.5	27250	27750
5.0	18250	19125
5.5	13150	13900
6.0	9550	10375
6.5	7200	7700
7.0	5650	6175
7.5	4440	4950
8.0	3465	3750
8.5	2725	2960
9.0	2160	2400
9.5	1720	1925
10.0	1375	1515
10.5	1120	1215
11.0	910	980
11.5	740	820
12.0	620	675
12.5	520	555
13.0	440	455
13.5	370	370
14.0	315	310
14.5	260	245

θ = scattering angle in degrees

I = current as counts in 10 seconds

Table 11.

Scattered Currents for the 8.35 Volt Excitation at 500 Volts

E = 508.80 volts, Pressure = 4.9×10^{-4} mm. Hg.,

Zero Angle for Run 1 = $1.20^{\circ} \pm 0.01^{\circ}$, Zero Angle for Run 2 = $1.32^{\circ} \pm 0.02^{\circ}$

θ	I Run 1	I Run 2
3.5	68850	67750
4.0	46550	43250
4.5	31175	29650
5.0	21025	20450
5.5	14525	14725
6.0	10400	10675
6.5	7875	7900
7.0	6100	5950
7.5	4760	4650
8.0	3675	3525
8.5	2885	2750
9.0	2250	2170
9.5	1775	1725
10.0	1390	1375
10.5	1090	1110
11.0	875	895
11.5	700	725
12.0	560	590
12.5	460	470
13.0	380	390
13.5	310	315
14.0	260	250
14.5	225	210
15.0	185	175

θ = scattering angle in degrees

I = current as counts in 10 seconds

Table 12

Scattered Currents for the 8.35 Volts Excitation at 600 Volts

E = 595.13 volts, Pressure = 4.9×10^{-4} mm. Hg.,
Zero Angle for Run 1 = 1.00° ± 0.01°, Zero Angle for Run 2 = 1.30° ± 0.01°

θ	I Run 1	I Run 2
3.0	104350	99000
3.5	65000	66250
4.0	42250	42400
4.5	29250	28500
5.0	19650	19150
5.5	14000	14150
6.0	10150	10000
6.5	7350	7200
7.0	5350	5250
7.5	4010	3850
8.0	3115	2955
8.5	2370	2290
9.0	1830	1785
9.5	1455	1405
10.0	1175	1110
10.5	930	885
11.0	730	710
11.5	605	570
12.0	495	460
12.5	400	380
13.0	330	305
13.5	270	250
14.0	250	210
14.5	200	190
15.0	175	150

θ = scattering angle in degrees

I = current as counts in 10 seconds

Table 13

Cross Sections of the 8.35 Volt Excitation of Carbon Monoxide at 420 Volts

E = 415.95 volts, W = 8.35 volts, $K = 3.358 \times 10^{-4}$,
$\alpha = 51$, $P = 4.9 \times 10^{-4}$ mm. Hg., $S_i = 2.914 \times 10^{-3} I \sin \theta$

θ	ΔP^2	I	S_i	$S_i \frac{Pm}{Pn} \Delta P^2$	f'_i
3.0	0.08656	93625	14.28	1.248	0.193
3.5	0.1167	60688	10.80	1.273	0.197
4.0	0.1514	40550	8.24	1.260	0.195
4.5	0.1908	27500	6.29	1.212	0.187
5.0	0.2348	18688	4.75	1.126	0.174
5.5	0.2834	13525	3.78	1.082	0.167
6.0	0.3366	9963	3.03	1.030	0.159
6.5	0.3944	7450	2.46	0.980	0.151
7.0	0.4569	5912	2.10	0.969	0.150
7.5	0.5238	4710	1.79	0.947	0.146
8.0	0.5956	3608	1.46	0.878	0.136
8.5	0.6718	2842	1.22	0.828	0.128
9.0	0.7526	2280	1.04	0.791	0.122
9.5	0.8379	1822	0.876	0.741	0.114
10.0	0.9280	1445	0.731	0.685	0.106
10.5	1.0224	1168	0.620	0.640	0.0989
11.0	1.1216	945	0.525	0.595	0.0919
11.5	1.2252	780	0.453	0.561	0.0867
12.0	1.3334	648	0.393	0.529	0.0817
12.5	1.4461	538	0.339	0.495	0.0764
13.0	1.5631	448	0.294	0.464	0.0717
13.5	1.6851	370	0.252	0.425	0.0656
14.0	1.8112	312	0.220	0.402	0.0621
14.5	1.9420	252	0.184	0.361	0.0558
15.0	2.0774				

Table 14.

Cross Sections of the 8.35 Volt Excitation of Carbon Monoxide at 500 Volts

E = 508.80 volts, W = 8.35 volts, $K = 3.358 \times 10^{-4}$,

$\alpha = 40$, $P = 4.9 \times 10^{-4}$ mm. Hg., $S_i = 2.107 \times 10^{-3} I \sin\theta$

θ	ΔP^2	I	S_i	$S_i \frac{Pm}{Pn} \Delta P^2$	f'_i
3.5	0.1417	68300	8.79	1.255	0.194
4.0	0.1842	44900	6.60	1.225	0.189
4.5	0.2324	30413	5.03	1.178	0.182
5.0	0.2864	20738	3.81	1.100	0.170
5.5	0.3460	14625	2.95	1.029	0.159
6.0	0.4112	10538	2.32	0.962	0.149
6.5	0.4820	7887	1.88	0.913	0.141
7.0	0.5585	6025	1.55	0.873	0.135
7.5	0.6406	4705	1.29	0.833	0.129
8.0	0.7285	3600	1.06	0.778	0.120
8.5	0.8219	2818	0.878	0.727	0.112
9.0	0.9209	2210	0.728	0.676	0.104
9.5	1.0255	1750	0.609	0.630	0.0973
10.0	1.1359	1382	0.506	0.579	0.0894
10.5	1.2515	1100	0.422	0.532	0.0822
11.0	1.3731	885	0.356	0.493	0.0762
11.5	1.5000	712	0.299	0.452	0.0698
12.0	1.6327	575	0.252	0.415	0.0641
12.5	1.7708	465	0.212	0.378	0.0584
13.0	1.9142	385	0.182	0.351	0.0542
13.5	2.0637	312	0.153	0.318	0.0491
14.0	2.2182	255	0.130	0.291	0.0450
14.5	2.3784	217	0.114	0.273	0.0422
15.0	2.5443	180	0.0982	0.252	0.0389

Table 15

Cross Sections of the 8.35 Volt Excitation of Carbon Monoxide at 600 Volts

E = 599.31 volts, W = 8.35 volts, $K = 3.358 \times 10^{-4}$,

$\alpha = 37$, $P = 4.9 \times 10^{-4}$ mm. Hg., $S_i = 1.728 \times 10^{-3} I \sin \theta$

θ	ΔP^2	I	S_i	$S_i \frac{Pm}{Pn} \Delta P^2$	f'_i
3.0	0.1227	101675	9.20	1.137	0.176
3.5	0.1663	65625	6.92	1.159	0.179
4.0	0.2164	42325	5.10	1.111	0.172
4.5	0.2732	28875	3.92	1.078	0.167
5.0	0.3369	19400	2.92	0.991	0.153
5.5	0.4071	14075	2.33	0.955	0.148
6.0	0.4840	10075	1.82	0.887	0.137
6.5	0.5676	7275	1.42	0.812	0.125
7.0	0.6578	5300	1.12	0.742	0.115
7.5	0.7546	3930	0.887	0.674	0.104
8.0	0.8582	3035	0.730	0.631	0.0975
8.5	0.9684	2330	0.595	0.580	0.0896
9.0	1.0852	1807	0.489	0.534	0.0825
9.5	1.2085	1430	0.408	0.497	0.0768
10.0	1.3387	1142	0.343	0.462	0.0714
10.5	1.4751	907	0.286	0.425	0.0656
11.0	1.6185	720	0.237	0.386	0.0596
11.5	1.7682	587	0.202	0.360	0.0556
12.0	1.9246	477	0.171	0.331	0.0511
12.5	2.0875	390	0.146	0.307	0.0474
13.0	2.2566	317	0.123	0.280	0.0433
13.5	2.4329	260	0.105	0.257	0.0397
14.0	2.6152	230	0.0962	0.253	0.0391
14.5	2.8041	195	0.0844	0.238	0.0367
15.0	2.9998	162	0.0725	0.219	0.0338

with ψ_o being the wave function for the ground state

ψ_i the wave function for the excited state

z_s the z coordinate of the s^{th} electron if the coordinate system is chosen with the z axis parallel to ΔP.

The inelastic scattering cross section is given by the Born approximation as

$$S_i \frac{Pm}{Pn} = \frac{4 |\mathcal{E}_i|^2}{\Delta P^4} \qquad (11)$$

Hence, combining this with equation (9),

$$f'_i = \frac{W_i}{2} S_i \frac{Pm}{Pn} \Delta P^2 \qquad (12)$$

Since S_i is a cross section per unit energy range, the oscillator strength, f'_i, defined above is in reality the oscillator strength per unit energy range and will be denoted throughout this dissertation as the "differential oscillator strength" to distinguish it from the integrated value of oscillator strength, f_i, which will be denoted by the term "oscillator strength," and which corresponds to the definition used in ultraviolet spectroscopy. This distinction has not heretofore been clearly made and it is hoped that this notation will help to eliminate confusion.

The limit of f'_i as $\Delta P^2 \rightarrow 0$ is the differential optical oscillator strength, and this quantity, when integrated over all rotational and vibrational energy losses associated with the electronic transition, gives the optical oscillator strength. Mulliken (32) has shown how the optical oscillator strength may be obtained from the integrated intensity curves of the ultra-violet absorption spectra and from dispersion measurements.

The differential oscillator strength for the 8.35 volt transition was obtained by extrapolation from Figure 20, a plot of f'_i as a function of ΔP^2, and is equal to 0.23. The extrapolation in this case is felt to be reliable because of the small curvature at small ΔP^2. The optical oscillator strength is obtained from the zero angle energy spectrum by integrating the differential oscillator strengths over the entire peak. The differential oscillator strength, f'_i, at energy loss, W_i, is determined from the equation

$$f'_i = \left(\frac{W_i}{W_j}\right)^3 \frac{I_i}{I_j} \quad f'_j \qquad (13)$$

where the j subscript refers to the maximum at 8.35 volts. These calculations are given in Table 16, resulting in an optical oscillator strength of 0.24. Unfortunately, no independent value could be found for comparison, but it is thought likely that other workers will carry out measurements

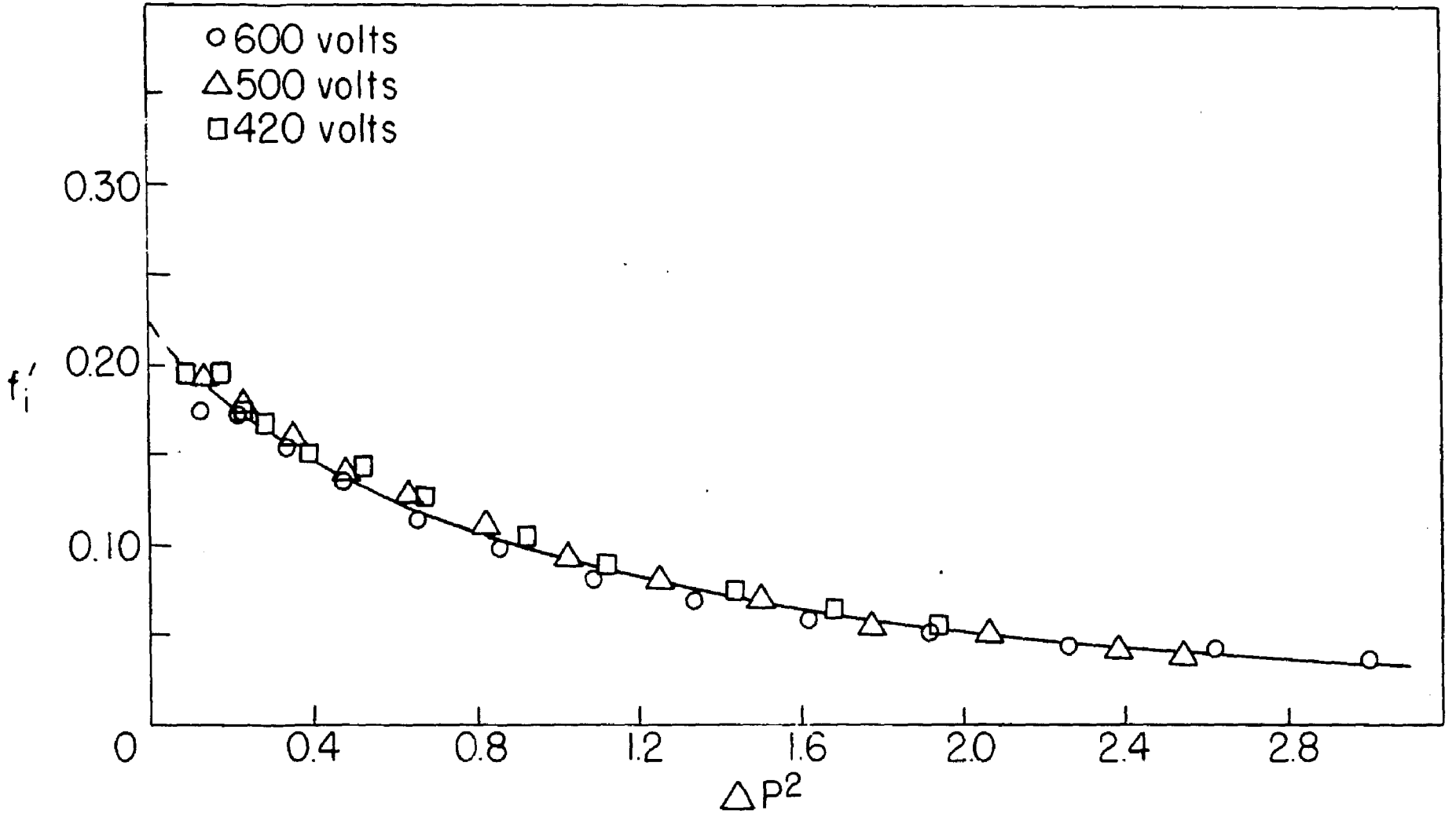

Figure 20. Differential Oscillator Strengths for the 8.35 Volt Transition in Carbon Monoxide

Table 16.

Optical Oscillator Strength of the 8.35 Volt Excitation of Carbon Monoxide

W_j = 8.35 volts, I_j = 102000 f'_j = 0.225

W_i	I_i	f_i'
7.35	2000	0.00301
7.45	3000	0.00470
7.55	3300	0.00538
7.65	4300	0.00729
7.75	8000	0.0141
7.85	15000	0.0275
7.95	32000	0.0609
8.05	49000	0.0969
8.15	66000	0.135
8.25	87000	0.185
8.35	102000	0.225
8.45	101000	0.231
8.55	97500	0.231
8.65	90500	0.222
8.75	80000	0.203
8.85	67000	0.176
8.95	55000	0.149
9.05	40000	0.112
9.15	28500	0.0827
9.25	21000	0.0630
9.35	15500	0.0480
9.45	12000	0.0384
9.55	9000	0.0297
9.65	6500	0.0221
9.75	5000	0.0176
9.85	4000	0.0145
9.95	3800	0.0142

Area 7.35 volt to 8.35 volt = 0.0649

Area 8.35 volt to 9.95 volt = 0.1760

Total Area = 0.241 = optical oscillator strength for the 8.35 volt excitation

on the absorption intensities of the ultraviolet spectra because of the great interest in the carbon monoxide molecule.

It should be noticed that if twice the integrated value for only one half the peak were taken as the oscillator strength, the result would be seriously in error. This is due to the fact that several vibrational states are involved in the excited molecule, which is apparent from the energy spectrum by the lack of symmetry of the peak. Hence it is evident that great care must be exercised in dealing with only partly resolved transitions in order to obtain reliable values of oscillator strengths. For the 11.41 volt transition, for example, the symmetry of the peak is good. A reliable value of oscillator strength could probably be obtained by integration from 11.4 to 11.2 volts. This calculation has not been carried out because of the uncertain value of the oscillator strength at $\Delta P^2 = 0$. (See following section.)

C. Angular Dependence of the 11.41 Volt Excitation

A single angular scattering run on the 11.41 volt transition was made at an accelerating voltage of 600 volts. Table 17 lists the experimental data as well as the calculated values of S_i, $S_i \frac{Pm}{Pn} \Delta P^2$, and f_i' for this run. Figure 19 shows the variation of the molecular cross section per unit energy range, S_i, as a function of the square of the change in momentum on impact ΔP^2, for this peak as well as for the 8.35 volt peak. It will be noted that the intensity of the 11.41 volt peak falls off much more rapidly with angle than that of the 8.35 volt peak, indicating a larger value of the matrix element of the dipole moment, $|\mathcal{E}_1|$.

A plot of the differential oscillator strength, f_i', as a function of ΔP^2 is given in Figure 21, from which an extrapolated value of the differential oscillator strength at $\Delta P^2 = 0$ has been obtained. This value, $f_i' = 0.43$ is very uncertain because of the large curvature at small ΔP^2. An additional estimate of f_i' may be obtained from the zero angle energy spectrum as follows. The differential oscillator strength is given by the equation

$$f_i' = \frac{W_i}{2} S_i \frac{Pm}{Pn} \Delta P^2 \qquad (14)$$

$$= \frac{W_i}{2} \frac{Ke^{\alpha Pl}}{PV(E-W_i)} \frac{I_i}{I_o} \left(\frac{E}{E-W_i}\right)^{1/2} \frac{(2E-W_i)}{2} \left[\sin^2 \frac{\theta}{2} + \left(\frac{W_i}{4E}\right)^2\right]$$

Table 17.

Cross Sections of the 11.41 Volt Excitation of Carbon Monoxide at 600 Volts

E = 599.31 volts, W = 11.41 volts, $K = 3.358 \times 10^{-4}$

$\alpha = 37$, $P = 4.9 \times 10^{-4}$ mm. Hg., $S_i = 1.737 \times 10^{-3} I \sin \theta$

θ	ΔP^2	I	S_i	$S_i \frac{Pm}{Pn} \Delta P^2$	f_i'
3.0	0.1243	106500	9.68	1.215	0.256
3.5	0.1677	57500	6.10	1.033	0.218
4.0	0.2178	29500	3.57	0.785	0.166
4.5	0.2745	15400	2.10	0.582	0.123
5.0	0.3380	9250	1.40	0.478	0.101
5.5	0.4080	5500	0.916	0.377	0.0796
6.0	0.4847	3100	0.563	0.276	0.0582
6.5	0.5681	1910	0.376	0.216	0.0456
7.0	0.6581	1315	0.278	0.185	0.0390
7.5	0.7546	965	0.219	0.167	0.0352
8.0	0.8580	740	0.179	0.155	0.0327
8.5	0.9678	610	0.157	0.153	0.0323
9.0	1.0843	545	0.148	0.162	0.0342

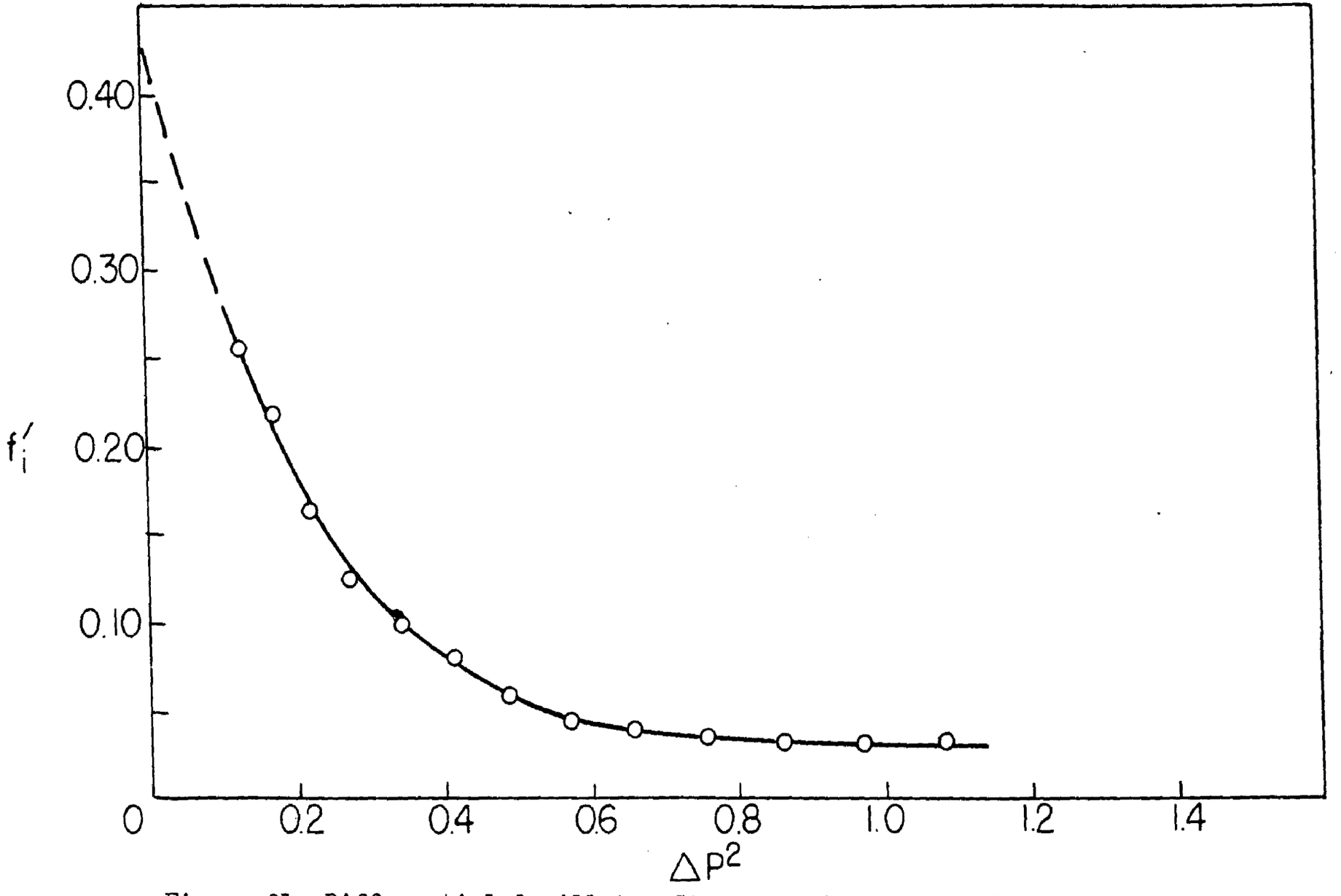

Figure 21. Differential Oscillator Strengths for the 11.41 Volt Transition in Carbon Monoxide

If we now take the ratio of the differential oscillator strength, f_i', at energy loss, W_i, to that of the differential oscillator strength f_j', at energy loss, W_j, at the zero scattering angle for the same pressure and accelerating voltage, we obtain

$$\frac{f_i'}{f_j'} = \left(\frac{W_i}{W_j}\right)^3 \quad \frac{I_i}{I_j} \quad \frac{2E - W_i}{2E - W_j} \quad \left(\frac{E - W_j}{E - W_i}\right)^{3/2} \tag{15}$$

In this case, the accelerating voltage was 508.8 volts, the current for the 8.35 volt transition was 102,000 counts in 10 seconds, the current for the 11.41 volt transition was 117,000 counts in 10 seconds, and the extrapolated value of the differential oscillator strength for the 8.35 volt transition was 0.225. Hence the calculated value of the differential oscillator strength for the 11.41 volt transition is 0.67, which may be compared with the value 0.43 obtained from the graphical extrapolation of Figure 21. This large difference is probably due primarily, as has been previously pointed out, to the difficulty of extrapolating the f_i' -- ΔP^2 curve. A more reliable value for the differential oscillator strength could be obtained by extending the cross section measurements to smaller angles, which could be done by replacing the present coarse slit (S_1 in Figure 1) by a slit with a smaller

width. Future work along these lines would be desirable as it would provide a better characterization of the excited states of the carbon monoxide molecule.

D. Cross Sections from Energy Spectra

For the presentation of the data dealing with the energy spectra, it was felt that the cross sections would be a more significant quantity than the current. If the ratio of cross sections at two different energy losses at the same scattering angle is taken, we obtain

$$S_i = \frac{I_i}{E-W_i} \left[\frac{(E-W_j}{I_j} \quad S_j \right] \tag{16}$$

The cross sections, S_j, of the 8.35 volt transition may be obtained from the currents, I_j, and the angular scattering curves, and these (S_j, I_j) are then used as the reference points for the determination of the cross sections, S_i, at various energy losses, W_i. These calculations are tabulated in Tables 18 to 23, where the cross sections, S_i, are given as a function of energy loss, W_i, at various scattering angles. In these calculations, the average value of $E - W_i$ was used for the energy loss ranges: 7.0 to 12.0 volts, 12.0 to 14.8 volts, and 14.8 to 18.0 volts. This introduces a negligible error into the final results.

Table 18.

Cross Sections from Energy Spectra at 500 Volts

Scattering Angle = 8.42°, E = 508.32 volts, $S_j\theta$ = 0.901

I_j = 2850, W_j = 8.35 volts

W_i	I_i	S_i	W_i	I_i	S_i
7.2	30	0.00947	13.0	1750	0.559
7.6	110	0.0347	13.1	1930	0.616
7.8	470	0.148	13.2	2070	0.661
8.0	1750	0.553	13.3	2200	0.703
8.2	2670	0.844	13.4	2350	0.751
8.35	2850	0.901	13.5	2400	0.766
8.5	2670	0.845	13.6	2300	0.735
8.6	2370	0.750	13.7	2200	0.703
8.8	1500	0.475	13.8	2150	0.687
9.0	850	0.269	13.9	2000	0.639
9.2	400	0.127	14.0	1850	0.591
9.4	230	0.0729	14.1	1750	0.559
9.6	150	0.0467	14.2	1600	0.511
9.8	120	0.0381	14.3	1530	0.489
10.0	100	0.0317	14.4	1430	0.457
10.2	80	0.0254	14.6	1270	0.406
10.4	120	0.0381	14.8	1120	0.360
10.6	340	0.108	15.0	1100	0.353
10.76	490	0.156	16.0	1120	0.360
10.9	360	0.114	16.1	1220	0.392
11.0	270	0.0858	16.2	1300	0.418
11.2	470	0.149	16.3	1320	0.424
11.3	620	0.197	16.4	1300	0.418
11.4	700	0.222	16.6	1250	0.402
11.5	630	0.200	16.7	1240	0.398
11.6	490	0.156	16.9	1340	0.431
11.8	220	0.0700	17.0	1380	0.443
11.9	120	0.0382	17.1	1400	0.450
12.0	170	0.0541	17.2	1370	0.440
12.2	430	0.137	17.4	1290	0.415
12.4	770	0.246	17.6	1200	0.386
12.5	850	0.271	17.8	1150	0.370
12.6	900	0.287	18.0	1120	0.360
12.7	1000	0.320	20.0	1120	0.363
12.8	1270	0.406	24.0	1070	0.349
12.9	1500	0.479	28.0	1020	0.336
			32.0	900	0.299

Table 19.

Cross Sections from Energy Spectra at 500 Volts

Scattering Angle = 7.32°, E = 508.32 volts, S_j = 1.39

I_j = 5100, W_j = 8.35 volts

W_i	I_i	S_i	W_i	I_i	S_i
7.0	30	0.00820	12.7	2050	0.563
7.2	40	0.0109	12.8	2430	0.667
7.4	100	0.0273	12.9	2830	0.777
7.6	320	0.0874	13.0	3500	0.961
7.8	1340	0.366	13.1	3830	1.05
8.0	3370	0.921	13.2	4050	1.11
8.1	4250	1.16	13.3	4200	1.15
8.2	5030	1.37	13.4	4250	1.17
8.35	5100	1.39	13.5	4250	1.17
8.5	4250	1.16	13.6	4170	1.15
8.6	3630	0.992	13.7	3930	1.08
8.7	2950	0.806	13.8	3650	1.00
8.8	2240	0.612	13.9	3470	0.953
9.0	1170	0.320	14.0	3300	0.906
9.2	550	0.150	14.1	3130	0.860
9.4	290	0.0792	14.2	2950	0.810
9.6	150	0.0410	14.3	2830	0.777
9.8	100	0.0273	14.4	2600	0.714
10.0	100	0.0273	14.6	2230	0.613
10.2	110	0.0301	14.8	2010	0.557
10.4	250	0.0683	15.0	2000	0.554
10.5	440	0.120	15.8	1960	0.543
10.6	740	0.202	16.0	2060	0.571
10.7	750	0.205	16.1	2290	0.634
10.8	670	0.183	16.2	2320	0.643
10.9	600	0.164	16.4	2350	0.651
11.0	510	0.139	16.6	2340	0.648
11.2	940	0.257	16.8	2280	0.632
11.3	1140	0.311	16.9	2370	0.657
11.4	1250	0.341	17.05	2640	0.731
11.5	870	0.238	17.2	2400	0.665
11.6	530	0.145	17.3	2280	0.632
11.8	200	0.0546	17.4	2180	0.604
11.9	200	0.0546	17.6	2020	0.560
12.0	370	0.101	17.8	1930	0.535
12.2	850	0.233	18.0	1900	0.526
12.4	1550	0.426	20.0	1850	0.516
12.5	1700	0.467	24.0	1770	0.498
12.6	1850	0.508	28.0	1660	0.471
			32.0	1410	0.403

Table 20.

Cross Sections from Energy Spectra at 500 Volts

Scattering Angle = 6.32°, E = 508.32 volts, S_j = 2.10,

W_j = 8.35 volts, I_j = 8800

W_i	I_i	S_i	W_i	I_i	S_i
7.0	40	0.00957	11.4	2700	0.646
7.2	40	0.00957	11.5	2200	0.526
7.4	100	0.0239	11.6	1450	0.347
7.6	320	0.0765	11.7	850	0.203
7.7	690	0.165	11.8	450	0.108
7.8	1300	0.311	11.9	400	0.0957
7.9	3250	0.777	12.0	470	0.112
8.0	5000	1.20	12.2	1350	0.325
8.1	6250	1.49	12.4	2670	0.644
8.2	7750	1.85	12.5	3200	0.771
8.35	8800	2.10	12.6	3550	0.856
8.5	8050	1.93	12.7	3930	0.947
8.6	6950	1.66	12.8	4650	1.12
8.7	5750	1.38	12.9	5350	1.29
8.8	4550	1.09	13.0	6400	1.54
8.9	3600	0.861	13.1	7150	1.72
9.0	2600	0.622	13.2	7850	1.89
9.1	1700	0.407	13.3	8350	2.01
9.2	1150	0.275	13.4	8600	2.07
9.4	600	0.144	13.5	8750	2.11
9.6	280	0.0670	13.6	8700	2.10
9.8	200	0.0478	13.7	8450	2.04
10.0	170	0.0407	13.8	7850	1.89
10.2	170	0.0407	13.9	7400	1.78
10.3	200	0.0478	14.0	7000	1.69
10.4	320	0.0765	14.1	6600	1.59
10.5	600	0.144	14.2	6130	1.48
10.6	1020	0.244	14.3	5850	1.41
10.7	1400	0.335	14.4	5300	1.28
10.77	1500	0.359	14.6	4550	1.10
10.9	1150	0.275	14.8	4250	1.03
11.0	980	0.234	15.0	4000	0.970
11.1	1260	0.301	15.5	3850	0.934
11.2	1900	0.454	16.0	4120	0.999
11.3	2550	0.610	16.1	4220	1.02

Table 20 (continued).

W_i	I_i	S_i
16.2	4300	1.04
16.3	4400	1.07
16.4	4500	1.09
16.5	4600	1.12
16.6	4400	1.07
16.7	4300	1.04
16.8	4500	1.09
16.9	4620	1.12
17.0	4820	1.17
17.1	5000	1.21
17.2	5000	1.21
17.3	4800	1.16
17.4	4580	1.11
17.6	4160	1.01
18.0	3750	0.910
20.0	3400	0.831
24.0	3200	0.788
28.0	2800	0.696
32.0	2220	0.556

Table 21.

Cross Sections from Energy Spectra at 500 Volts

Scattering Angle = 5.41°, E = 508.32 volts, S_j = 3.02

I_j = 15600, W_j = 8.35 volts

W_i	I_i	S_i	W_i	I_i	S_i
7.0	35	0.00679	11.44	8500	1.65
7.2	35	0.00679	11.5	7600	1.47
7.4	100	0.0194	11.6	5200	1.01
7.6	500	0.0970	11.7	3200	0.621
7.7	1100	0.213	11.8	1600	0.310
7.8	2200	0.427	11.9	900	0.175
7.9	4500	0.873	12.0	900	0.175
8.0	8400	1.63	12.2	2600	0.509
8.1	11300	2.19	12.4	5600	1.10
8.2	14200	2.76	12.5	6900	1.35
8.35	15600	3.02	12.6	8200	1.60
8.5	14800	2.87	12.7	8900	1.74
8.6	13300	2.58	12.8	10200	1.99
8.7	11100	2.15	12.9	11700	2.99
8.8	8800	1.71	13.0	13500	2.64
8.9	7100	1.38	13.1	15500	3.03
9.0	5500	1.07	13.2	18300	3.58
9.1	4000	0.776	13.3	18800	3.68
9.2	2500	0.485	13.4	18800	3.68
9.4	1300	0.252	13.5	18400	3.60
9.6	600	0.116	13.6	18000	3.52
9.8	400	0.0776	13.7	17800	3.48
10.0	200	0.0388	13.8	16700	3.27
10.2	200	0.0388	13.9	15800	3.09
10.3	400	0.0776	14.0	15000	2.93
10.4	600	0.116	14.1	14400	2.82
10.5	900	0.175	14.2	13600	2.66
10.6	2000	0.388	14.3	12300	2.41
10.7	2700	0.524	14.4	11300	2.21
10.80	3200	0.621	14.6	9700	1.90
10.9	2700	0.524	14.8	8600	1.69
11.0	2400	0.466	15.0	8600	1.69
11.1	3000	0.582	15.5	8300	1.63
11.2	4900	0.951	15.8	7800	1.53
11.3	6500	1.26	16.0	8100	1.59
11.4	8100	1.57	16.1	8400	1.65

Table 21 (continued).

W_i	I_i	S_i
16.2	8700	1.71
16.3	8900	1.75
16.4	9100	1.79
16.5	9100	1.79
16.6	9000	1.77
16.7	8800	1.73
16.8	9200	1.81
16.9	10000	1.97
17.0	10200	2.01
17.1	10000	1.97
17.2	9500	1.87
17.3	9300	1.83
17.4	9000	1.77
17.6	8400	1.65
17.8	8100	1.59
18.0	7700	1.52
20.0	6800	1.35
24.0	6200	1.24
28.0	5100	1.03
32.0	3900	0.793

Table 22.

Cross Sections from Energy Spectra at 500 Volts

Scattering Angle = 4.58°, S_j = 4.48, I_j = 28500

W_j = 8.35 volts, E = 508.80 volts

W_i	I_i	S_i	W_i	I_i	S_i
7.0	75	0.0118	11.5	14200	2.24
7.2	150	0.0236	11.6	9200	1.45
7.4	450	0.0709	11.7	5900	0.930
7.6	1900	0.299	11.8	3000	0.473
7.7	3600	0.567	11.9	1900	0.299
7.8	7800	1.23	12.0	2200	0.347
7.9	12800	2.02	12.2	5800	0.921
8.0	19300	3.04	12.4	12600	2.00
8.1	24200	3.81	12.5	14600	2.32
8.2	27400	4.32	12.6	16200	2.57
8.35	28500	4.48	12.7	18800	2.99
8.5	26100	4.11	12.8	20800	3.30
8.6	20800	3.28	12.9	24400	3.87
8.7	17600	2.77	13.0	27600	4.38
8.8	14400	2.27	13.1	31200	4.95
8.9	10300	1.62	13.2	34400	5.46
9.0	8000	1.26	13.3	34800	5.53
9.1	5500	0.867	13.4	34800	5.53
9.2	3900	0.614	13.5	35400	5.62
9.4	1800	0.284	13.6	36000	5.72
9.6	1000	0.158	13.7	32800	5.21
9.8	500	0.0788	13.8	31200	4.95
10.0	400	0.0630	13.9	30000	4.76
10.2	600	0.0945	14.0	27800	4.41
10.3	900	0.142	14.1	25400	4.03
10.4	1700	0.268	14.2	24000	3.81
10.5	3000	0.473	14.3	22400	3.56
10.6	4000	0.630	14.4	20600	3.27
10.7	5300	0.835	14.6	18400	2.92
10.75	6000	0.945	14.8	16400	2.62
10.8	5400	0.851	15.0	16000	2.56
10.9	5000	0.788	15.5	15300	2.44
11.0	6400	1.01	15.8	15000	2.40
11.1	9000	1.42	16.0	15000	2.40
11.2	12400	1.95	16.1	15300	2.44
11.3	18800	2.96	16.2	15700	2.51
11.33	19000	2.99	16.33	16000	2.56
11.4	18500	2.91	16.4	15800	2.52

Table 22 (continued).

W_i	I_i	S_i
16.5	15600	2.49
16.6	15700	2.51
16.7	16200	2.59
16.8	16500	2.64
16.9	16900	2.70
17.0	17200	2.75
17.1	17400	2.78
17.2	17000	2.72
17.3	16200	2.59
17.4	15600	2.49
17.6	14700	2.35
17.8	13800	2.20
18.0	12800	2.05
20.0	11600	1.87
24.0	10600	1.72
28.0	8700	1.42
32.0	6700	1.11

Table 23.

Cross Sections from Energy Spectra at 500 Volts

Scattering Angle = 3.42°, S_j = 9.20, I_j = 72200

E = 508.32 volts, W_j = 8.35 volts

W_i	I_i	S_i	W_i	I_i	S_i
7.0	200	0.0255	11.5	61000	7.79
7.2	800	0.102	11.6	40500	5.17
7.4	1200	0.153	11.7	23000	2.94
7.6	4000	0.511	11.8	12500	1.60
7.7	8200	1.05	11.9	6000	0.766
7.8	15000	1.92	12.0	6000	0.766
7.9	31500	4.02	12.2	16300	2.10
8.0	49500	6.32	12.4	36000	4.63
8.1	60500	7.73	12.5	46500	5.99
8.2	68300	8.72	12.6	55000	7.08
8.35	72200	9.20	12.7	60000	7.72
8.5	70800	9.04	12.8	69300	8.92
8.6	61500	7.86	12.9	76000	9.78
8.7	50000	6.39	13.0	83000	10.69
8.8	39700	5.07	13.1	90300	11.63
8.9	31000	3.96	13.2	97800	12.59
9.0	23800	3.04	13.3	102000	13.13
9.1	16000	2.04	13.4	100300	12.91
9.2	11500	1.47	13.5	99000	12.75
9.4	5000	0.639	13.6	98000	12.62
9.6	2000	0.255	13.7	92500	11.91
9.8	1200	0.153	13.8	83000	10.69
10.0	800	0.102	13.9	80500	10.36
10.2	1000	0.128	14.0	78500	10.11
10.3	1200	0.153	14.1	71000	9.14
10.4	2800	0.358	14.2	63000	8.11
10.5	5000	0.639	14.3	60000	7.72
10.6	10000	1.28	14.4	55500	7.15
10.7	13500	1.72	14.6	48000	6.18
10.8	14300	1.83	14.8	48000	6.22
10.9	16000	2.04	15.0	46500	6.02
11.0	22500	2.87	15.5	44300	5.74
11.1	33500	4.28	15.8	43000	5.57
11.2	49000	6.26	16.0	42000	5.44
11.3	64500	8.24	16.1	43000	5.57
11.4	75000	9.58	16.2	44000	5.70

Table 23 (continued).

W_i	I_i	S_i
16.3	45000	5.83
16.4	45200	5.85
16.5	45300	5.87
16.6	45200	5.85
16.7	45800	5.93
16.8	46500	6.02
16.9	47200	6.11
17.0	48000	6.22
17.1	48300	6.26
17.2	48000	6.22
17.3	46200	5.98
17.4	44300	5.74
17.6	39500	5.12
17.8	37000	4.79
18.0	38000	4.92
19.0	32000	4.17
20.0	32000	4.18
24.0	25000	3.29
28.0	19000	2.52
32.0	13500	1.81

(E) Elastic Cross Sections

The elastic collision cross sections have been determined at an accelerating voltage of 600 volts over an angular range from 10 to 90 degrees. The experimental results for σ_E and $\sigma_E \Delta P^2$ are presented in Table 24. A theoretical calculation of these cross sections may be made by use of the Born Approximation, which gives for the elastic cross section

$$\sigma_E = \frac{4\,|\mathcal{E}|^2}{\Delta P^4} \qquad (17)$$

where $\mathcal{E}$ is given by (33)

$$\mathcal{E} = \sum_j (Z_j - f_j)\, e^{i\vec{\Delta P} \cdot \vec{r}_j} \qquad (18)$$

where

Z_j = charge on nucleus j

f_j = scattering factor for nucleus j

$\vec{\Delta P}$ = vector change in momentum

$\vec{r}_j$ = vector from an arbitrary origin to nucleus j.

Hence

$$\mathcal{E}\mathcal{E}^* = \sum_j \sum_k (Z_j - f_j)(Z_k - f_k)\, e^{i\vec{\Delta P} \cdot \vec{r}_{jk}} \qquad (19)$$

where

$\vec{r}_{jk}$ = vector from atom j to atom k.

On integrating this expression over all orientations of $\vec{r}_{jk}$ to the incident electron beam we obtain

$$|\mathcal{E}|^2 = \overline{\mathcal{E}\mathcal{E}^*} = \sum_j \sum_k (Z_j - f_j)(Z_k - f_k) \frac{\sin \Delta P R_{jk}}{\Delta P\ R_{jk}} \qquad (20)$$

Table 24.

Elastic Cross Sections at 600 Volts

$b = 0.563$, $E = 598.80$, $P = 4.9 \times 10^{-4}$ mm. Hg, $\alpha = 37$

$K = 3.358 \times 10^{-4}$

θ	ΔP^2	I	σ_E	$\sigma_E \Delta P^2$
10.0	1.3449	102000	17.01	22.88
10.5	1.4821	85750	15.01	22.25
11.0	1.6264	71500	13.10	21.31
11.5	1.7770	61500	11.77	20.92
12.0	1.9344	53250	10.63	20.56
12.5	2.0983	46150	9.59	20.13
13.0	2.2684	39800	8.60	19.50
13.5	2.4458	34200	7.67	18.75
14.0	2.6292	29400	6.83	18.22
15.0	3.0162	22300	5.54	16.72
16.0	3.429	17400	4.60	15.79
17.0	3.868	14000	3.93	15.20
18.0	4.332	11450	3.40	14.72
19.0	4.822	9500	2.97	14.32
20.0	5.337	8200	2.69	14.37
22.0	6.446	6250	2.25	14.49
24.0	7.653	4850	1.90	14.50
26.0	8.958	3850	1.62	14.52
28.0	10.361	3100	1.40	14.47
30.0	11.859	2530	1.22	14.41
32.0	13.451	2040	1.04	13.96
34.0	15.132	1625	0.873	13.21
36.0	16.904	1270	0.717	12.12
38.0	18.765	975	0.576	10.81
40.0	20.709	775	0.478	9.90
45.0	25.924	495	0.336	8.71
50.0	31.619	375	0.276	8.73
55.0	37.744	295	0.232	8.76
60.0	44.257	225	0.187	8.28
65.0	51.108	180	0.157	8.02
70.0	58.242	145	0.131	7.63
75.0	65.607	120	0.111	7.28
80.0	73.148	95	0.0898	6.57
85.0	80.796	100	0.0957	7.73
90.0	88.514	100	0.0960	8.50

where ΔP = magnitude of $\vec{\Delta P}$

R_{jk} = internuclear distance from atom j to atom k.

For the diatomic molecule carbon monoxide substitution of this equation into equation (17) gives

$$\sigma_E = \frac{4\,|\varepsilon|^2}{\Delta P^4} = \frac{4}{\Delta P^4}\left\{(Z_c-f_c)^2+(Z_o-f_o)^2+2(Z_c-f_c)(Z_o-f_o)\,\frac{\sin \Delta PR}{\Delta PR}\right\} \tag{21}$$

Scattering factors calculated from Slater wave functions are given as a function of ΔP by Berman (21). Calculated values of the elastic cross sections and of $\sigma_E \Delta P^2$ are given in Table 25, and Figure 22 shows the comparison between the calculated and experimental values of cross sections. It will be noticed that a crossover occurs at small values of ΔP^2. This effect has previously been noted for Helium (34), Argon (21), and Nitrogen (19), the theoretical values being considerably lower than the experimental at values of ΔP^2 much smaller than those in this investigation, and has been attributed to polarization caused by the incident electron. In the intermediate range of ΔP^2, the discrepancy is of the order of magnitude of 25 percent. This is not surprising inasmuch as the calculations assume a spherically symmetric charge distribution around each atom, a condition which is certainly non-existent in a heteronuclear molecule such as

Table 25.

Theoretical Elastic Cross Sections

$R = 1.128 \times 10^{-8}$ cm. = 2.132 a.u.

ΔP	ΔP^2	f_c	f_o	σ_E	$\sigma_E \Delta P^2$
1.0	1.00	4.491	6.712	21.92	21.92
1.2	1.44	4.029	6.242	16.33	23.52
1.4	1.96	3.590	5.749	11.91	23.35
1.6	2.56	3.195	5.255	8.67	22.19
1.8	3.24	2.855	4.775	6.44	20.87
2.0	4.00	2.570	4.322	4.975	19.90
2.2	4.84	2.338	3.904	4.062	19.66
2.4	5.76	2.153	3.529	3.449	19.87
2.6	6.76	2.006	3.195	3.009	20.34
2.8	7.84	1.891	2.906	2.647	20.75
3.0	9.00	1.799	2.657	2.320	20.88
4.0	16.00	1.534	1.893	0.972	15.55
5.0	25.00	1.364	1.630	0.364	9.10
6.0	36.00	1.201	1.429	0.201	7.24
8.0	64.00	0.8897	1.195	0.0668	4.28
10.0	100.00	0.6360	0.9695	0.0322	3.22

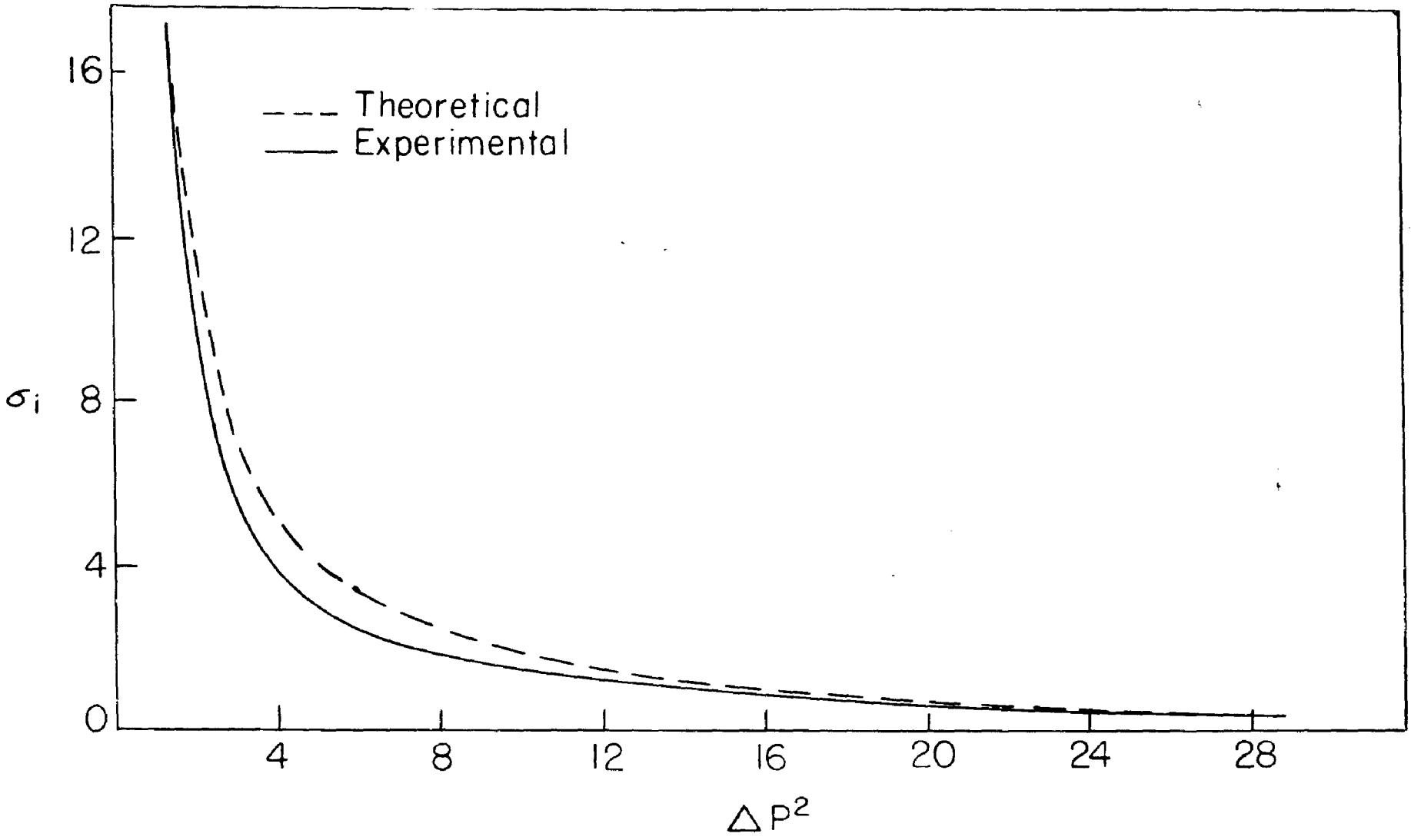

Figure 22. Theoretical and Experimental Cross Sections for Carbon Monoxide

carbon monoxide. At wide angles (e.g. large ΔP^2), the calculated and experimental results approach each other, as is expected, since the wide angle scattering is primarily due to the inner shell electrons whose charge distribution is much more nearly spherically symmetric.

IV. On the Structure of Carbon Monoxide

Since the early days of the theory of valency, the structure of carbon monoxide has presented a problem as the classical valency of four for carbon and two for oxygen cannot be reconciled with the existence of the molecule. With the advent of wave mechanics, several attempts were made to set up structures which would be in accord with the experimental facts, notably in connection with the interpretation of the ultraviolet spectrum. In this section, an attempt will be made to see whether the data obtained in this investigation can be used to judge the relative merits of some of these interpretations.

Mulliken (15) in 1932 discussed the ultraviolet spectrum in detail. A summary of this evidence and some later spectroscopic work will be presented here. The term symbol for the ground state of CO has been found to be $^1\Sigma^+$. The term symbols for the ground state and the first two excited states of ionized carbon monoxide, CO^+, have been shown to be $^2\Sigma^+$, $^2\Pi$, and $^2\Sigma^+$, respectively. Tanaka et. al. in 1942 (35) (36) found Rydberg Series of bands from the ground state of CO to these three states of CO^+ with ionization potentials of 13.944, 16.454, and 19.577 volts, respectively. Hence

from symmetry considerations the three states of CO^+ may be obtained by excitation of an electron from σ, π, and σ molecular orbitals of the ground state of CO. From the ionization potential evidence these orbitals, in order of increasing energy, are $y\sigma$, $w\pi$, and $x\sigma$, the notation being that of Mulliken. The first excited state of CO is $^1\pi$, the second and third are $^1\Sigma^+$. Hence, from symmetry, the next two molecular orbitals may be denoted by $v\pi$, and $u\sigma$, the $u\sigma$ orbital having the higher energy. Taken all together, this evidence gives us the electron configuration postulated by Mulliken,

$$(K)\ (K)\ \ (Z\sigma)^2\ (y\sigma)^2\ (w\pi)^4\ (x\sigma)^2$$

with the orbitals being arranged from left to right in order of increasing energy. For this assignment, it is not necessary to specify the combinations of atomic orbitals making up the molecular orbitals or the bonding character of the individual molecular orbitals.

A short summary of the electron scattering and spectroscopic data for the first three excitations of CO and for the states of CO^+ will be useful at this point. Table 26 lists the observed energy losses on electron impact, the spectroscopic energy difference between ground state and excited state, the spectroscopic internuclear distance, and the intensities

relative to the 8.35 volt peak obtained from the zero angle energy spectrum. The spectroscopic data are taken from the compilation by Herzberg (30).

Table 26.

Data for the Ground and Excited States of CO and CO^+

	Energy Loss-Electron Impact - volts	State	Energy Loss-Spectroscopic - volts	Internuclear Distance Angstroms	Rel. Intensity Electrical Impact
CO:	0	$X^1\Sigma^+$	0	1.128	---
	8.35	$A^1\Pi$	8.05	1.235	1.00
	10.78	$B^1\Sigma^+$	10.76	1.120	0.11
	11.41	$C^1\Sigma^+$	11.38	1.125	1.16
CO^+:	---	$X^2\Sigma^+$	13.94	1.115	---
	---	$A^2\Pi$	16.45	1.244	---
	---	$B^2\Sigma^+$	19.58	1.169	---

The relative intensities as a function of angle have been given previously in Table 7, where it is seen that the 8.35 volt and 10.78 volt transitions vary in approximately the same way, both being radically different from the 11.41 volt transition. In addition, the half-width of the 8.35 volt peak is of the order of one volt and that of the 11.41 volt peak, at smaller angles, is of the order of 0.5 volt. The half-width of the latter peak is thus comparable to that of an atomic transition. From the angular scattering curves, one would also expect that, qualitatively, at least, the

the matrix element of the dipole moment for this transition is considerably larger than those for the other two transitions. A comparison of the oscillator strengths for the 8.35 volt and 11.41 volt transitions leads to the same conclusion.

Mulliken (15) specifies the bonding character of the orbitals as follows: (K) is an orbital for the inner shell electrons, the ($z\sigma$), ($w\pi$) and ($x\sigma$) are bonding orbitals, and the ($y\sigma$) is an anti-bonding orbital. This classification is the same as that for the isoelectronic molecule nitrogen and would lead one to expect similar behavior for the two molecules. The next two higher orbitals are the anti-bonding orbitals ($v\pi$) and ($u\sigma$), again as in nitrogen. The classification outlined above gives a satisfactory explanation for the first excited state, $A^1\pi$, which corresponds to the excitation of an electron from a bonding ($x\sigma$) orbital to an anti-bonding ($v\pi$) orbital with a consequent increase in the internuclear distance. The next two transitions expected would correspond to excitations of an electron from the bonding ($x\sigma$) orbital to the anti-bonding ($u\sigma$) orbital and from the bonding ($w\pi$) orbital to the anti-bonding ($v\pi$) orbital, both giving rise to $^1\Sigma^+$ states with increased internuclear distance. It is at this point, as Mulliken has pointed out, that the

classification scheme breaks down, since the internuclear distances of both these states are shorter than in the ground state. In addition, the oscillator strengths for these two states should be much larger than that for the $A^1\Pi$ state (see ref. (30), page 381 ff. and references cited therein), while rough calculations using data from the zero angle energy spectrum indicate that the oscillator strengths for the 8.35 volt transition ($A^1\Pi$) and the 11.41 volt transition ($C^1\Sigma^+$) are approximately the same ($\simeq 0.25$) and that for the 10.78 volt transition ($B^1\Sigma^+$) is about one-tenth of these. Hence it is clear that the molecular orbital classification outlined by Mulliken does not give a satisfactory over-all picture for carbon monoxide.

Long and Walsh (37), in giving a general relationship between the polarity of the carbonyl group and ionization potential, consider the molecule to consist of a double bond between the carbon and oxygen atoms, an unshared pair of electrons on the carbon atom, and two unshared pairs on the oxygen atom, this being a situation closely analogous to that of aldehydes and ketones (38) (39). A comparison of the energy spectra of carbon monoxide with those of acetone and methyl ethyl ketone (see Appendix) indicates clearly that this is not the case. In addition, theoretical calculations by McMurry (39) show that oscillator strengths

to be expected for transitions of this type are of the order of magnitude of 0.01 - 0.03, which are much lower than experimentally determined in this investigation. Experimentally determined oscillator strengths for these transitions in ketones are lower than 0.01.

Moffitt (16) has considered the problem from the viewpoint of molecular orbital theory and writes the ground state configuration as

$$(K)(K)(s\sigma)^2(t\sigma)^2(w\pi)^4(u\sigma)^2$$

where (K) corresponds to an inner shell pair of electrons, ($s\sigma$) to an unshared pair on the oxygen atom, ($t\sigma$) to a bonding pair, ($w\pi$) to a bonding orbital with four electrons, and ($u\sigma$) to an unshared pair on the carbon atom. The next highest orbital is an anti-bonding ($v\pi$) orbital. This configuration is similar to that of Mulliken (15), differing only in the specific assignment of the atomic orbitals which make up the molecular orbitals. The $A^1\Pi$ transition is now considered to arise from the excitation of a non-bonding ($u\sigma$) electron to the anti-bonding orbital ($v\pi$), leading to an increased internuclear distance. The $B^1\Sigma^+$ transition is assumed to arise from the excitation of a non-bonding ($u\sigma$) orbital to a Rydberg orbital ($r\sigma$), larger than the

rest of the molecule, thus producing a structure essentially that of CO^+ which is known to have a shorter internuclear distance than CO.

The argument outlined above does not explain the large oscillator strength of the $A^1\Pi$ transition, since a sub-Rydberg transition of this type is expected to have a low oscillator strength (see ref. (30), page 385). In addition, no explanation for the $C^1\Sigma^+$ state is given.

Thus it is seen that all of the proposed electron configurations are unsatisfactory in one way or another. A complete molecular orbital treatment would be very tedious and has not been carried out. An unsuccessful attempt was made to see if any qualitative differences between a $\sigma - \sigma$ and $\pi - \pi$ transition could be found without knowing the specific form of the molecular orbitals. Quantitative theoretical calculations of the scattering cross sections and oscillator strengths must therefore be deferred until such time as plausible molecular orbitals for the ground state and excited states of the molecule are available.

A final comment on the similarity of carbon monoxide and nitrogen may be made here. Scattering cross sections for nitrogen have been determined by Krasnow (40) who has also

observed the optically forbidden transition corresponding to the $A^1\Pi$ transition of carbon monoxide. If the electron configurations for both molecules are similar, then symmetry considerations would lead one to expect that those moments in the expansion of $|\varepsilon|^2$ which vanish for Nitrogen would be small for Carbon Monoxide and hence the oscillator strength for this transition in carbon monoxide would be small. That this is not the case experimentally shows that a fundamental difference in the two molecules exists.

SUMMARY

Energy spectra have been obtained at several accelerating voltages and over a wide range of scattering angles. The excitation potentials and the manner in which their relative intensity varies with scattering angle are reported. In addition, the collision cross sections at energy losses over a range of 30 volts have been calculated from these spectra and are presented in tabular form.

An intensive investigation of the inelastic collision cross sections of the 8.35 volt transition between 4 and 15 degrees at incident electron energies of 420, 500, and 600 volts has been carried out. The Born approximation has been found to give a satisfactory explanation of these results. Differential oscillator strengths as a function of ΔP^2 and the optical oscillator strength have been calculated for this transition.

The inelastic collision cross sections for the rapidly varying transition at 11.41 volts were determined from a single run at 600 volts. Differential oscillator strengths were calculated from this data and compared with the oscillator strength at $\Delta P^2 = 0$ calculated from the energy spectrum at zero scattering angle.

Elastic cross sections have been determined from 10 to 90 degrees scattering angle and have been compared with a theoretical calculation based on Slater wave functions. The theoretical and experimental curves cross over at two points, one at small and one at large values of ΔP^2. In the intermediate range differences of the order of magnitude of 25 percent in the numerical values of the calculated and experimental cross sections are found.

Several proposed models for the bonding of carbon monoxide have been discussed. It was concluded that there is as yet no plausible model which can be used as a basis for semi-quantitative theoretical calculations of cross sections and oscillator strengths.

APPENDIX: ENERGY SPECTRA OF ACETONE AND METHYL ETHYL KETONE

Wide angle and zero angle energy spectra of acetone and methyl ethyl ketone were obtained at approximately 220 volts and 500 volts, and are shown in Figures 23 to 30. The experimental conditions for these spectra are summarized in Table 27. The gas pressure for all runs was 2.1×10^{-4} mm. Hg.

Table 27.

EXPERIMENTAL CONDITIONS FOR KETONE ENERGY SPECTRA

Compound	Figure	Acc. Volts	Foc. Volts	Slit Bias-Volts	Beam Current-Micro Amperes	Scattering Angle - Degrees
Acetone	23	220	-165	270	3.14	6.5
Acetone	24	500	-395	0	3.14	6.5
Acetone	25	220	-165	---	0.15	0
Acetone	26	500	-395	0	0.15	0
M.E.K.	27	220	0	270	3.14	7
M.E.K.	28	500	0	0	3.14	7
M.E.K.	29	220	0	270	3.14	0
M.E.K.	30	500	0	0	0.31	0

The change in the appearance of these spectra from zero angle to wide angle is quite remarkable, particularly for acetone, as can be seen from a comparison of Figures 24 and 26. For both ketones a region of almost continuous absorption begins at about 7.3 volts with a large number of electronic states so close together than any attempts at location of these states on the basis of so few spectra could easily be misleading. At the zero scattering angle in acetone, however,

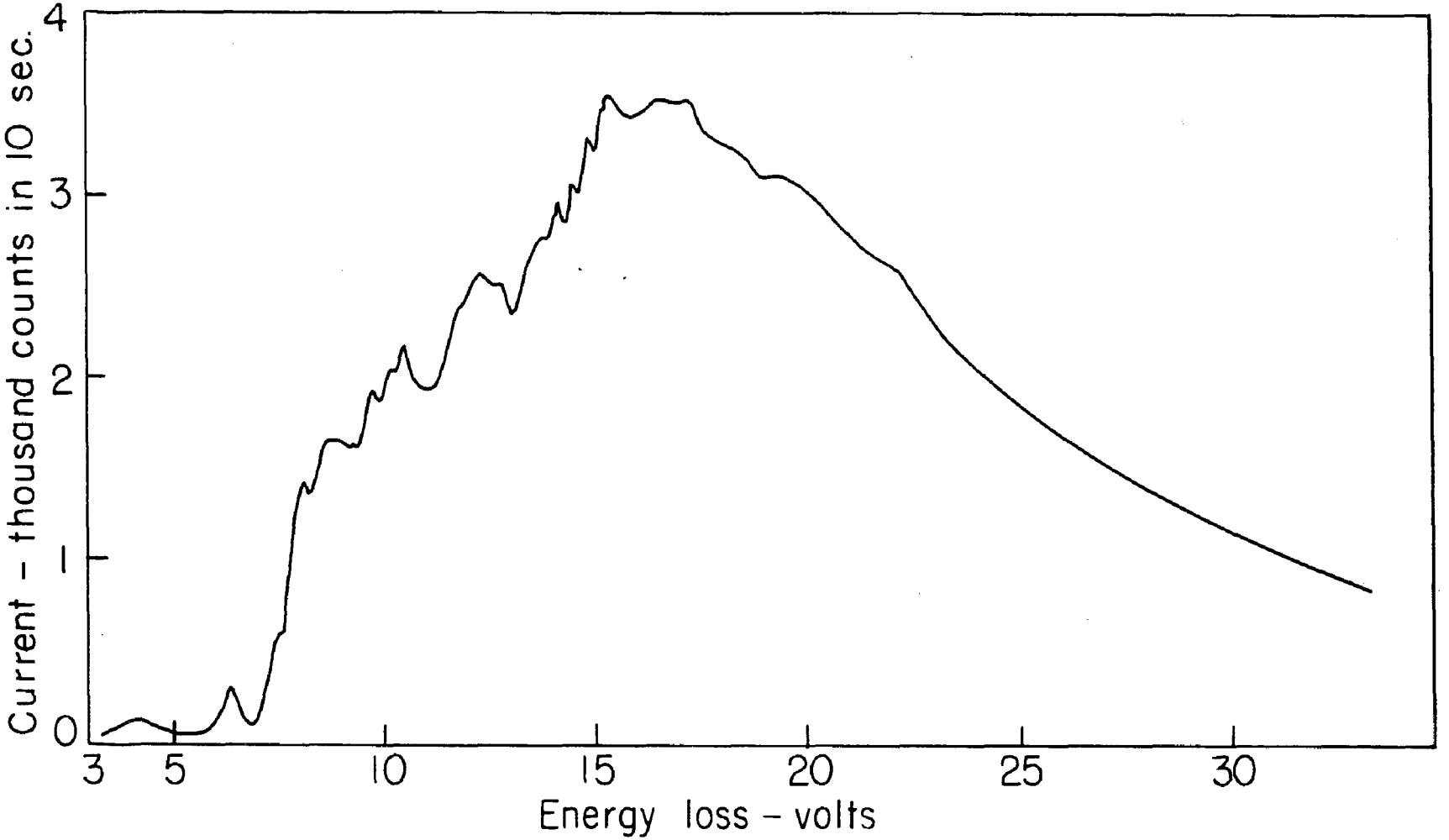

Figure 23. Energy Spectrum of Acetone at 220 Volts and Scattering Angle 6.5°

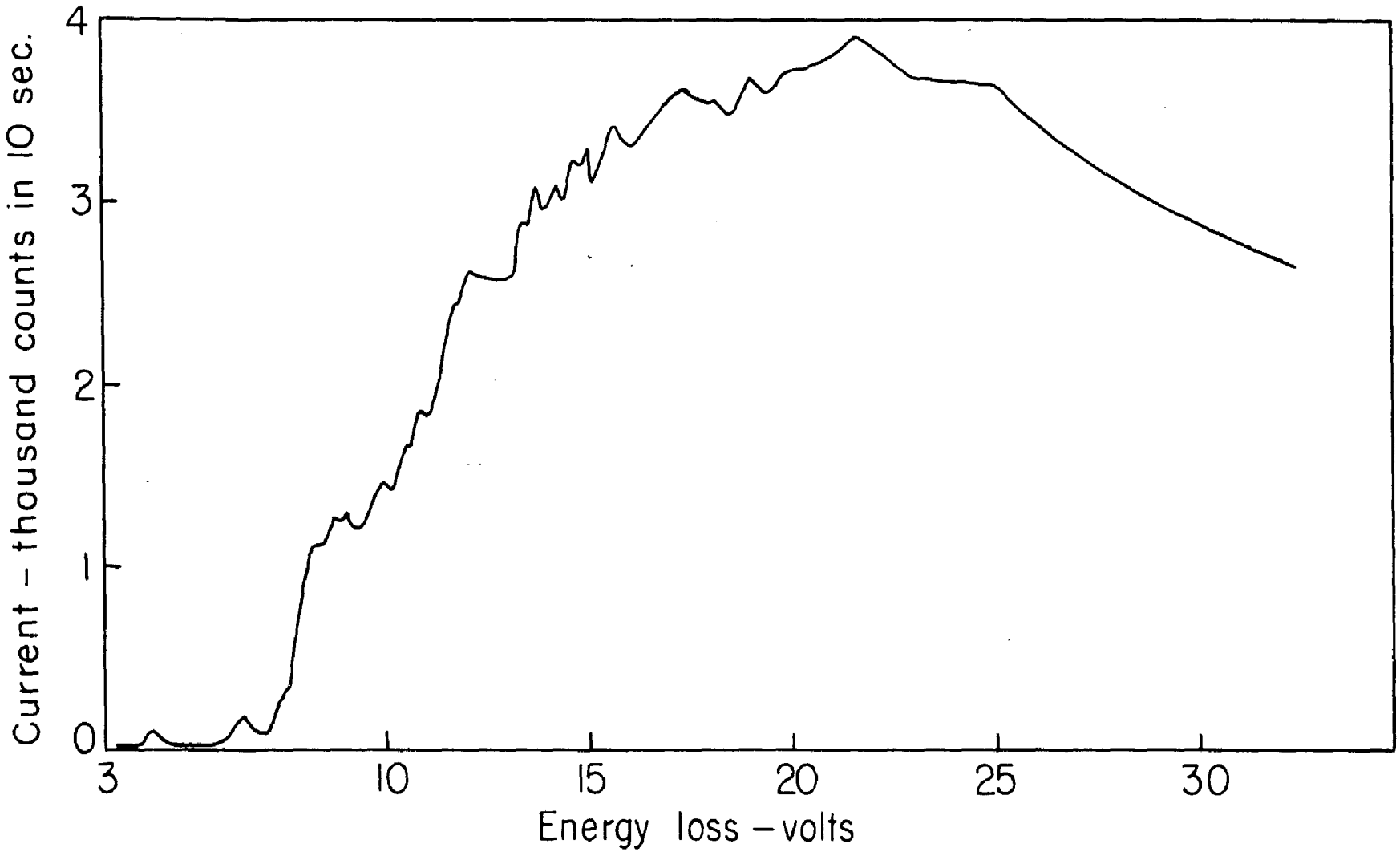

Figure 24. Energy Spectrum of Acetone at 500 Volts and Scattering Angle 6.5 °

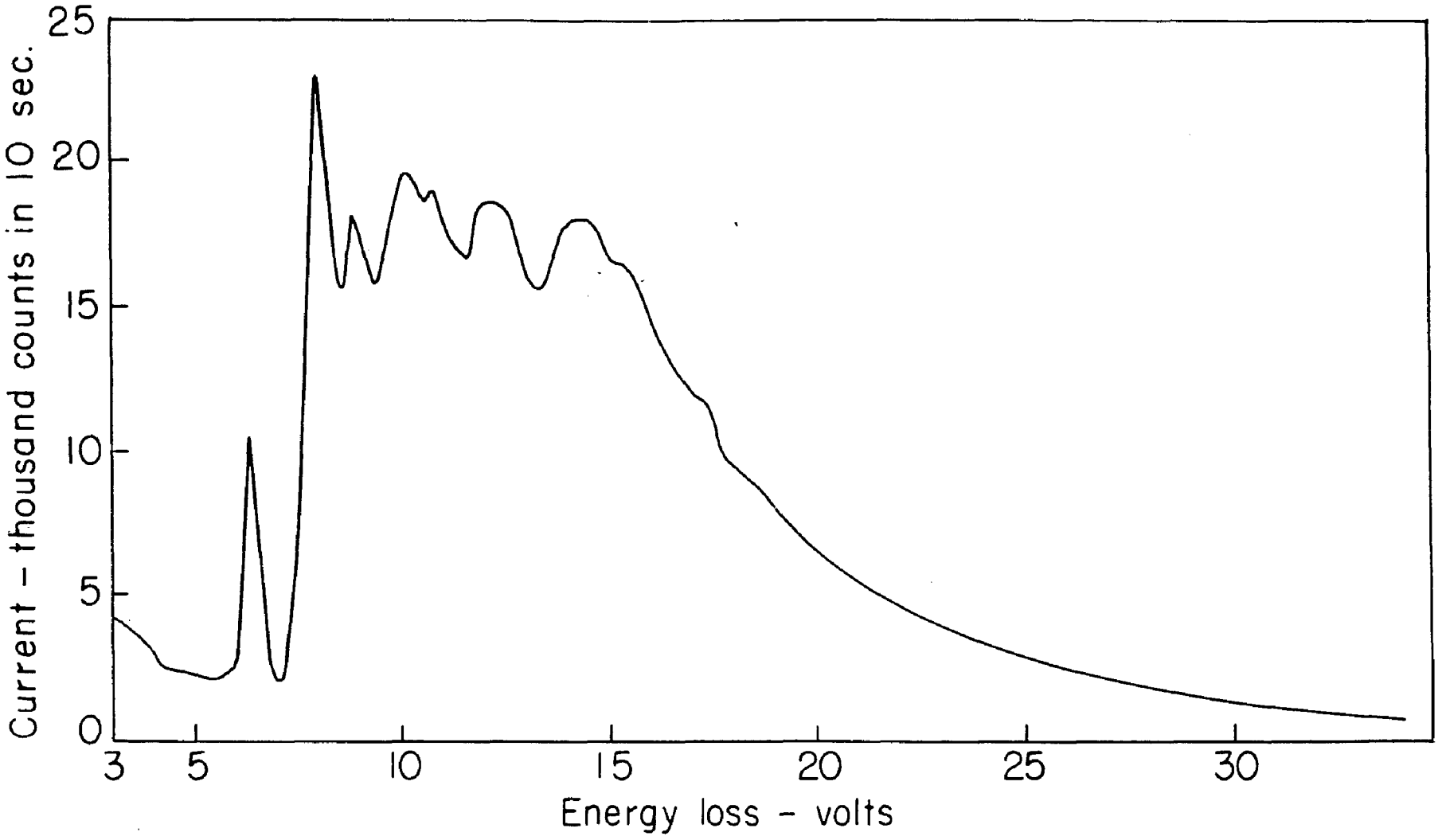

Figure 25. Energy Spectrum of Acetone at 220 Volts and Scattering Angle Zero Degrees

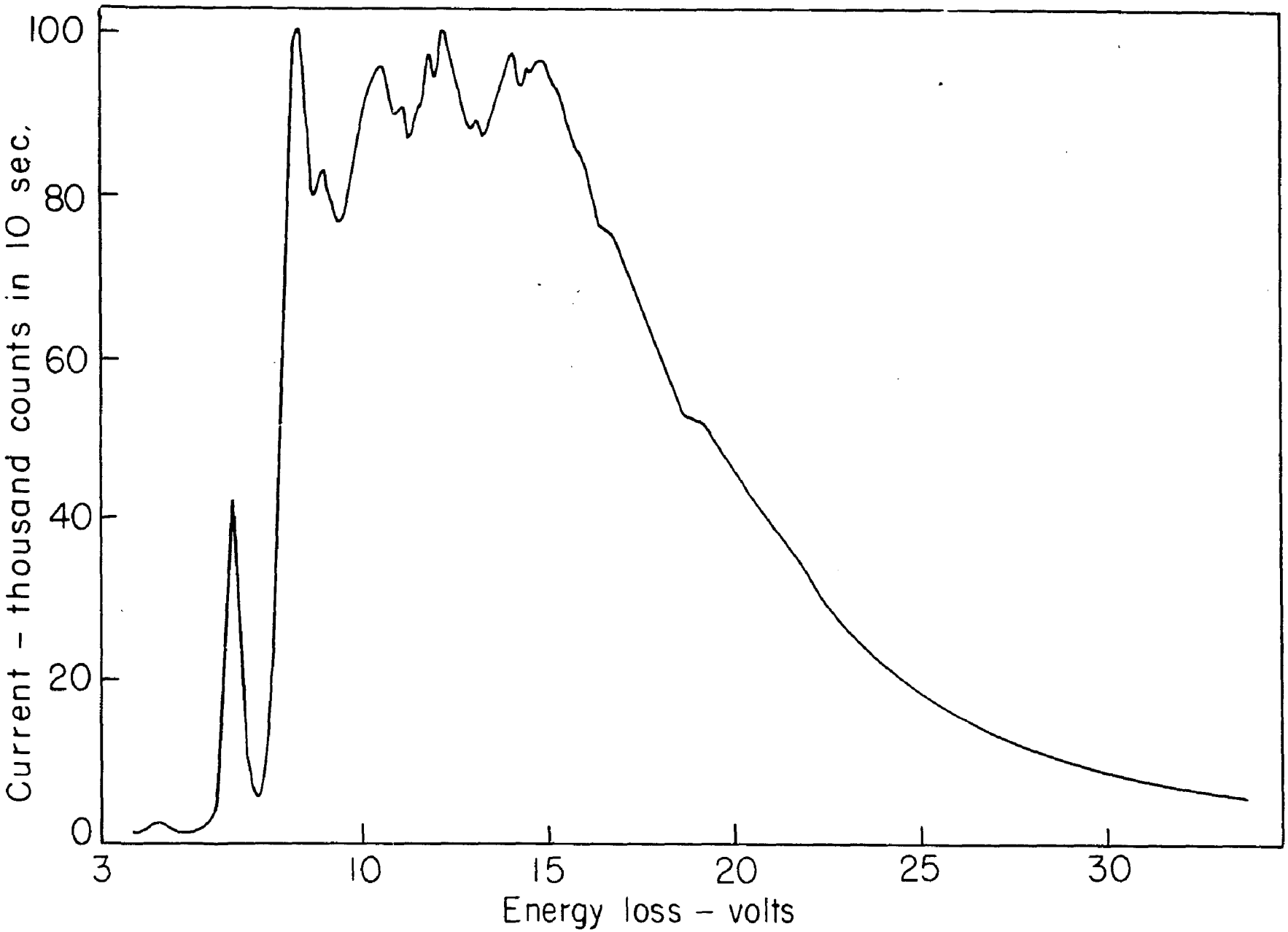

Figure 26. Energy Spectrum of Acetone at 500 Volts and Scattering Angle Zero Degrees

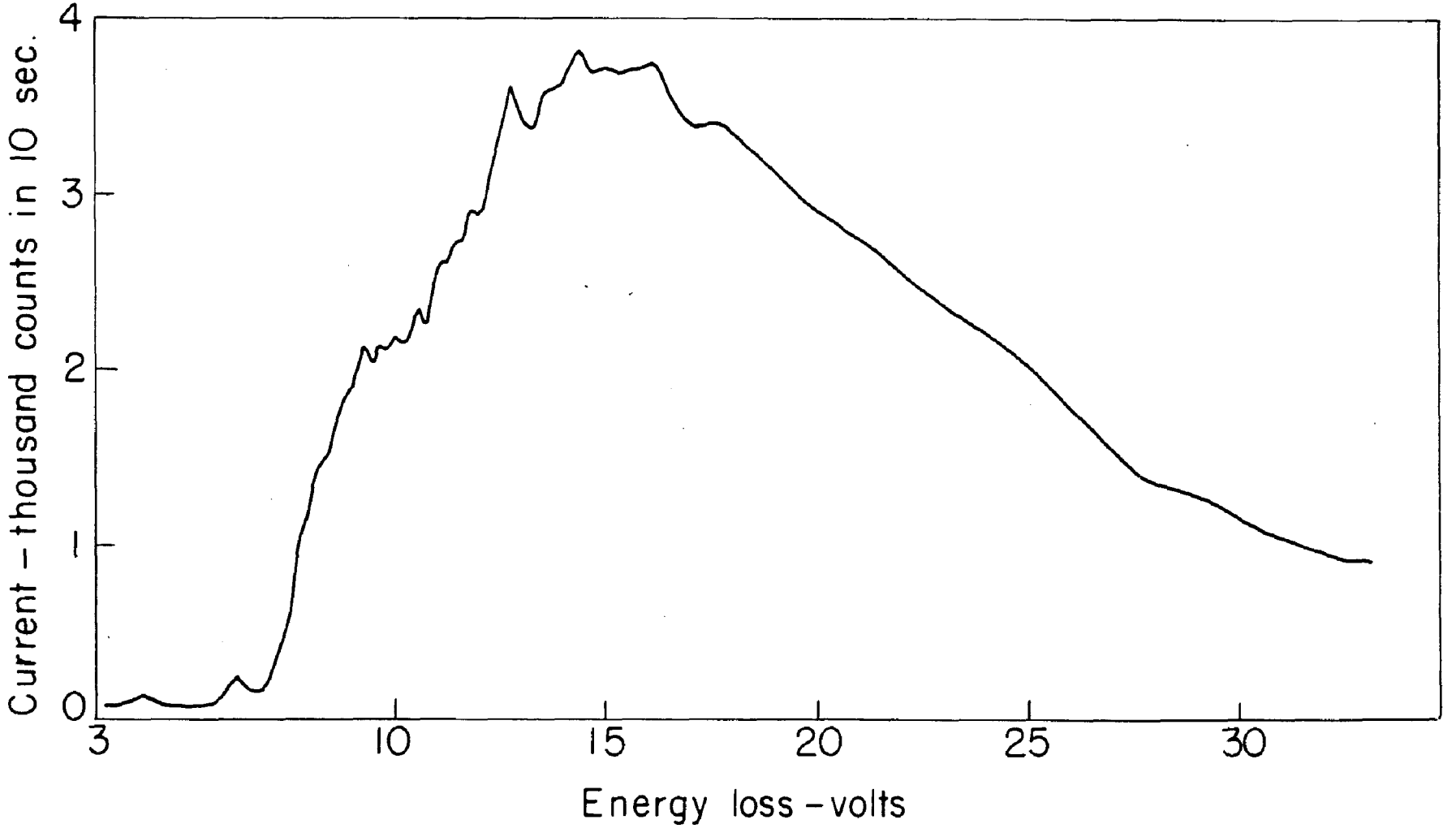

Figure 27. Energy Spectrum of Methyl Ethyl Ketone at 220 Volts and Scattering Angle 7 Degrees.

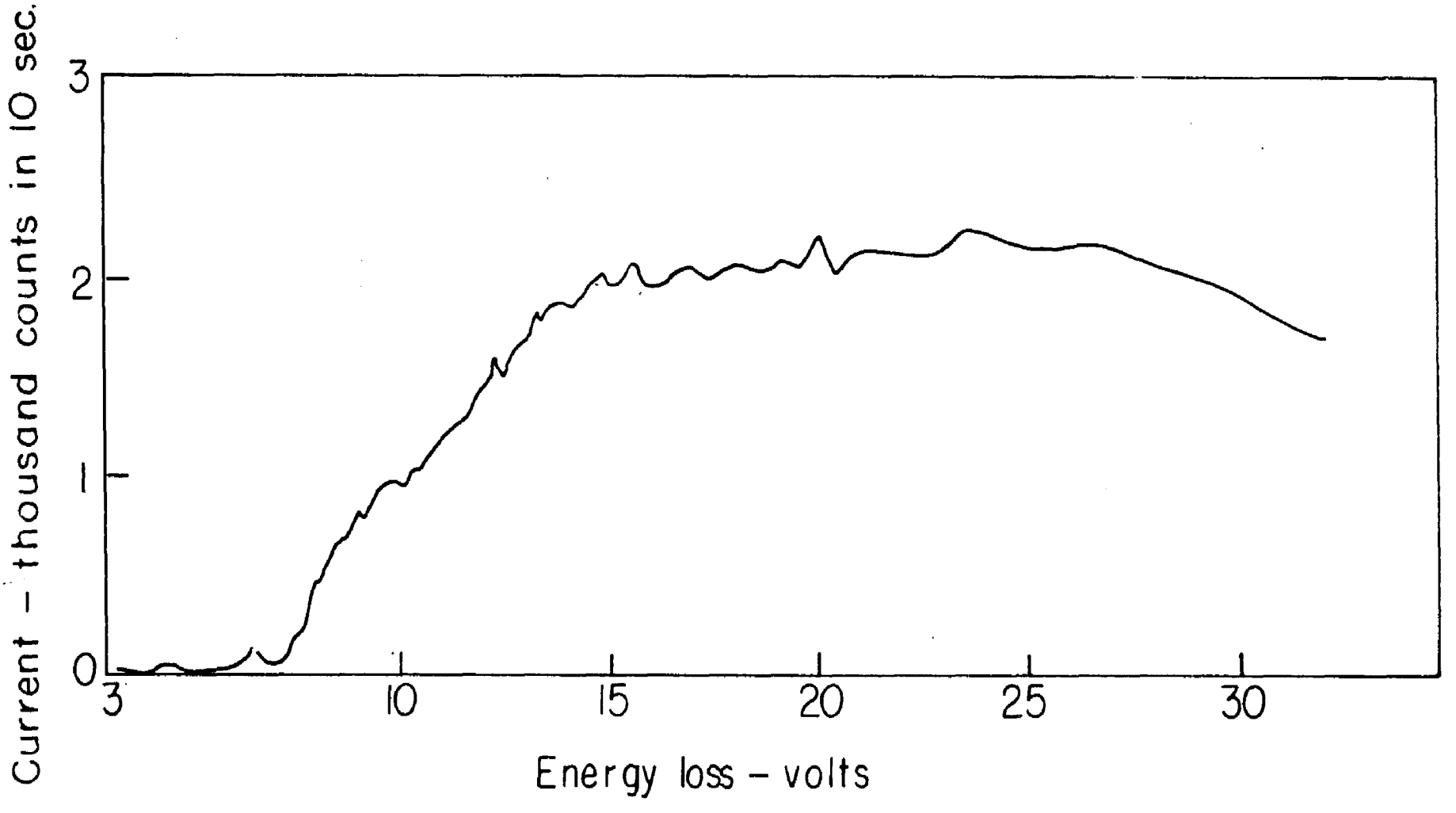

Figure 28. Energy Spectrum of Methyl Ethyl Ketone at 500 Volts and Scattering Angle 7 Degrees

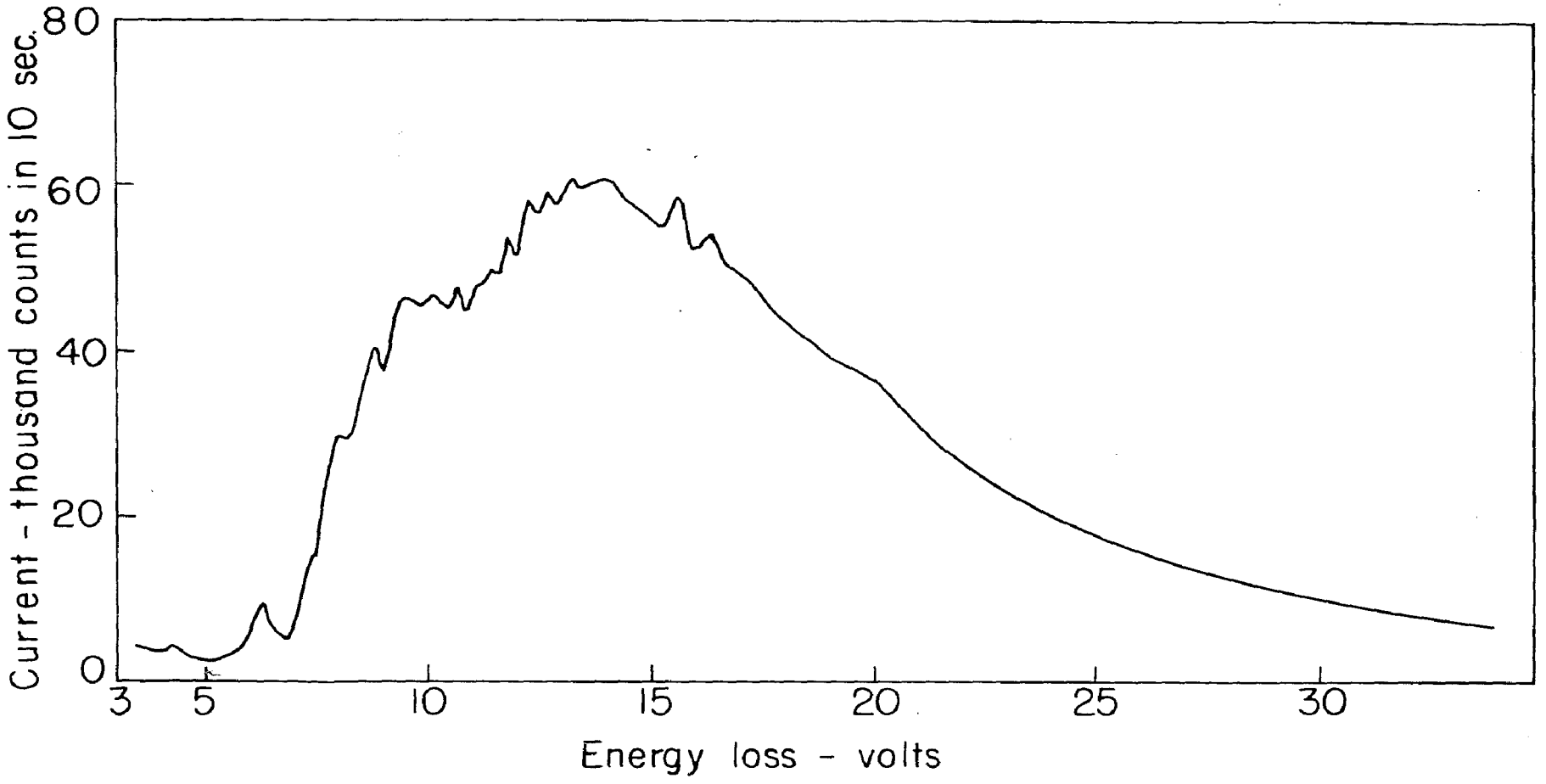

Figure 29. Energy Spectrum of Methyl Ethyl Ketone at 220 Volts and Scattering Angle Zero Degrees

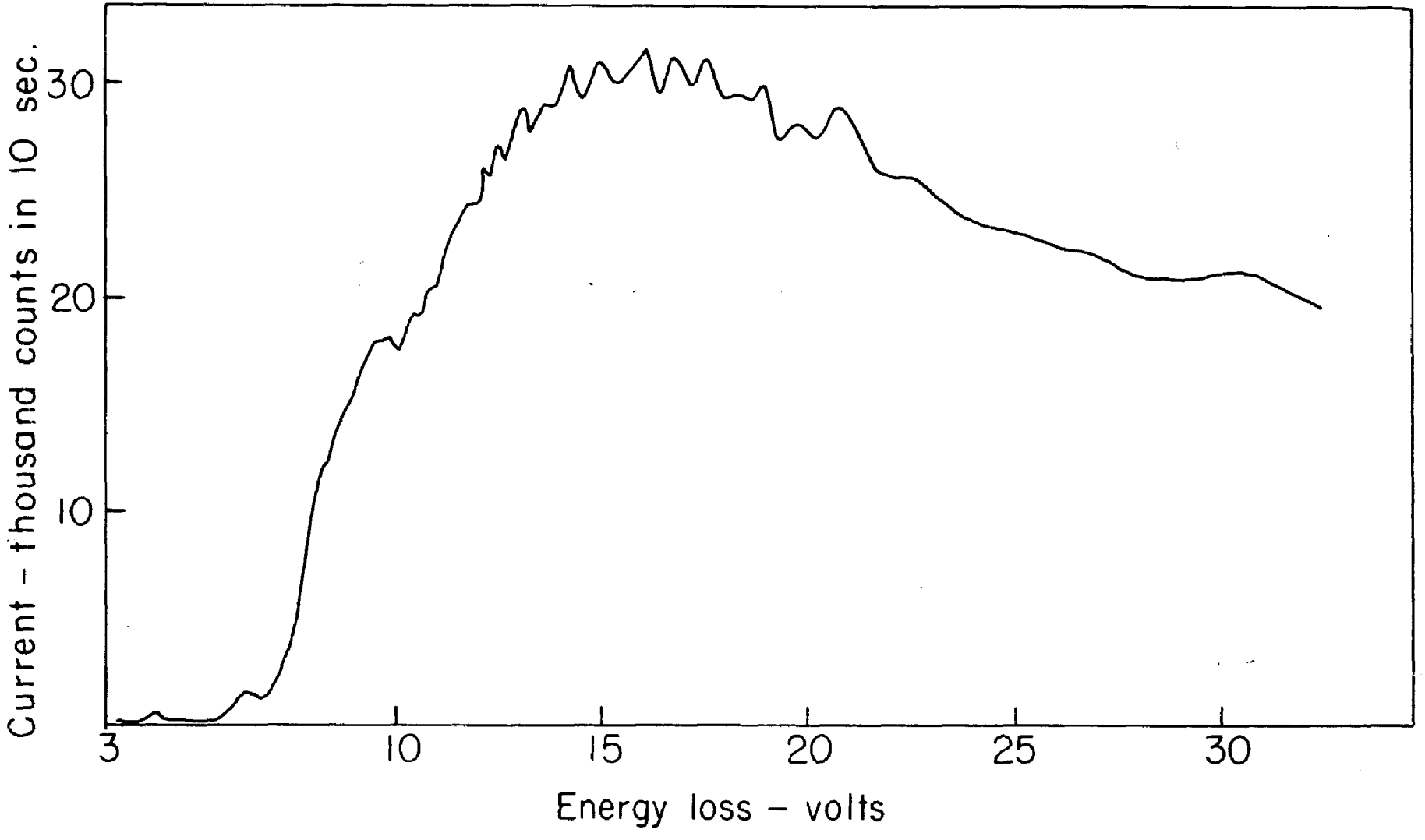

Figure 30. Energy Spectrum of Methyl Ethyl Ketone at 500 Volts and Scattering Angle Zero Degrees

several of these peaks become very intense, in particular, those at 8.1, 8.8, 10.3, 10.9, 12.2, and 14.2 volts. The behavior of the continuum is also very interesting inasmuch as at the wider angles the scattered currents in the continuum are larger than those for any of the discrete peaks in the spectrum. This effect has previously been observed to a smaller extent by Edmisten (22) in his study of ethane and methane and by John (20) in methane. A satisfactory explanation of this phenomenon has not been found and a more comprehensive angular study would be desirable.

Two peaks common to both ketones occur in these spectra. In acetone these occur at 4.3 and 6.4 electron-volts and in methyl ethyl ketone at 4.2 and 6.4 electron-volts. These correspond to well-known transitions in the ultraviolet spectra which have been ascribed to excitations in the carbonyl bond. Mulliken (38) and McMurry (39) consider both peaks to be due to excitation of an electron from a non-bonding unshared pair on the oxygen atom to anti-bonding orbitals in the bond, the 4.2 volt transition being forbidden and the 6.4 volt transition being allowed. The energy spectra given here support this view since the intensity of the 4.2 volt peaks relative to the background and the 6.4 volt peak is smaller at the zero scattering angle than at the wide angle. For a more rigorous proof

of the forbidden nature of the 4.2 volt peak a comprehensive study of the energy spectra as a function of scattering angle would have to be carried out.

Duncan and collaborators (41), (42), (43), (44) and Scheibe, Povenz and Linstrom (45) have studied the ultraviolet spectra of ketones. Duncan has reported weak bands between 7.45 and 7.90 volts, strong bands from 8.07 to 8.30 volts, increasingly strong continuous absorption with some band structure from 8.58 to 9.65 volts, and strong continuous absorption from 9.65 to 15.5 volts. These results are in qualitative agreement with those reported here.

BIBLIOGRAPHY:

(1) P.D. Foote and E.L. Mohler, Phys. Rev. 17, 394 (1921); ibid. 29, 141 (1927)

(2) J. Savard and M. de Hemptinne, Compt. Rend. 204, 354 (1927); ibid. 206, 998 (1938): J. Phys. Radium 10, 30 (1939)

(3) W. Harries, Z. Physik 42, 26 (1927)

(4) H. Lohner, Ann. Physik 24, 349-60 (1935)

(5) H.L. Brose and E.H. Saayman, Ann. Physik (5) 5, 797 (1930)

(6) C. Ramsauer and R. Kollath, Ann. Physik (5) 4, 91 (1930)

(7) E. Bruche, Ann. Physik 83, 1065 (1927)

(8) R.B. Brode, Phys. Rev. 25, 636 (1925)

(9) C.E. Normand, Phys. Rev. 35, 1217 (1930)

(10) E. Rudberg, Proc. Roy. Soc. (London) A130, 182 (1930)

(11) E. Rudberg, Ann. Physik 11, 802 (1931)

(12) R. Kollath, Ann. Physik 87, 259 (1928)

(13) C. Ramsauer and R. Kollath, Ann. Physik 12, 529 (1932)

(14) F.L. Arnot, Proc. Roy. Soc. (London) A133, 615 (1931)

(15) R.S. Mulliken, Rev. Mod. Physics 4, 1 (1932)

(16) W.E. Moffitt, Proc. Roy. Soc. (London) A196, 524 (1949)

(17) S.A. Francis, Ph.D. Dissertation, The Ohio State University (1947)

(18) E.A. Jones, Ph.D. Dissertation, The Ohio State University, (1948)

(19) L.B. Dean, Ph.D. Dissertation, The Ohio State University, (1949)

(20) G.S. John, Ph.D. Dissertation, The Ohio State University, (1949)

BIBLIOGRAPHY (CONTINUED)

(21) A.S. Berman, Ph.D. Dissertation, The Ohio State University, (1949)

(22) W.C. Edmisten, Ph.D. Dissertation, The Ohio State University, (1949)

(23) G.M. Begun, Ph.D. Dissertation, The Ohio State University, (1950)

(24) Yarnold and Bolton, J. Sci. Instr. 26, 38 (1949)

(25) J.S. Allen, Rev. Sci. Instr. 18, 739 (1947)

(26) Jordan and Bell, Rev. Sci. Instr. 18, 703 (1947)

(27) Womer, Phys. Rev. 45, 689 (1934)

(28) Dreisbach and Martin, Ind. Eng. Chem. 41, 2875, (1949)

(29) Timmermans, Bull. Soc. Chim. Belg. 44, 17 (1935)

(30) G. Herzberg, Molecular Spectra and Molecular Structure, vol. I., Spectra of Diatomic Molecules, D. Van Nostrand Co., Second Edition, 1950

(31) Bethe, Ann. Physik 5, 325 (1930)

(32) Mulliken and Rieke, Repts. Progress Physics 8, 231 (1941) (and references cited therein)

(33) Brockway, Rev. Mod. Physics 8, 231 (1936)

(34) Mott and Massey, Theory of Atomic Collisions, Oxford: Clarendon Press, Second Edition (1949)

(35) Y. Tanaka, Sci. Papers Inst. Phys. Chem. Research (Tokyo) 39, 447 (1942)

(36) T. Takamine, Y. Tanaka and M. Iwata, Sci. Papers Inst. Phys. Chem. Research (Tokyo) 40 371 (1943)

(37) L.H. Long and A.D. Walsh, Trans. Faraday Soc. 43, 342 (1947)

(38) R.S. Mulliken, J. Chem. Phys. 3, 564 (1935)

BIBLIOGRAPHY (CONTINUED)

(39) H.L. McMurry, J. Chem. Phys. 9, 231 (1941)

(40) M.E. Krasnow, Ph.D. Dissertation, The Ohio State University, (1952)

(41) A.B.F. Duncan, J. Chem. Phys. 8, 444 (1940)

(42) A.B.F. Duncan, J. Chem. Phys. 3, 131 (1935)

(43) Duncan, Ells and Noyes, J. Amer. Chem. Soc. 58, 1454, (1936)

(44) Noyes, Duncan and Manning, J. Chem. Phys. 2, 717 (1934)

(45) Scheibe, Povenz and Linstrom, Zeits. f. Physik. Chemie B20, 283 (1933)

AUTOBIOGRAPHY

I, Sam Silverman, was born in New York City on November 16, 1925. I received my secondary school education in the public schools of New York City. My undergraduate training was obtained at the City College of the College of the City of New York from which I received the degree Bachelor of Chemical Engineering in 1945. I was admitted to The Ohio State University in 1947. While in residence at this university, I was awarded an assistantship during 1948 and again from 1949 to 1951. I received an appointment as University Scholar for the academic year 1948-49. Since July, 1951, I have served as Research Fellow under the auspices of the Research Foundation, while completing the requirements for the degree Doctor of Philosophy.